Molecular Pharmacology Fast Forward. Published on October 9, 2008 as doi:10.1124/mol.108.051490

TITLE PAGE

Title: Amitriptyline Activates Cardiac Ryanodine Channels And Causes Spontaneous Sarcoplasmic Reticulum Calcium Release

Authors: Nagesh Chopra, Derek Laver, Sean S. Davies, Bjorn C. Knollmann

Affiliation: Oates Institute for Experimental Therapeutics and Division of Clinical Pharmacology, Departments of Medicine and Pharmacology, Vanderbilt University Medical Center, Nashville, TN (N.C., S.S.D., B.C.K); Department of Biomedical Sciences, University of Newcastle and HMRI, Callaghan, Australia (D.L.).

Molecular Pharmacology Fast Forward. Published on October 9, 2008 as DOI: 10.1124/mol.108.051490
This article has not been copyedited and formatted. The final version may differ from this version.

RUNNING TITLE PAGE

Running title: Amitriptyline activates RyR2 channels

Address correspondence to:

Björn C. Knollmann, M.D., Ph.D., Associate Professor of Medicine and Pharmacology, Oates Institute for Experimental Therapeutics, Division of Clinical Pharmacology, Vanderbilt University Medical Center, 1265 Medical Research Building IV, Nashville, TN 37232-0575

Office: (615) 343-6493, fax: (615) 343-4522, e-mail: bjorn.knollmann@vanderbilt.edu

Number of text pages: 26

Number of tables: 1

Number of figures: 12

Number of references: 40

Number of words in Abstract: 250

Number of words in Introduction: 415

Number of words in Discussion: 1203

Nonstandard abbreviations used in the manuscript: AMT: amitriptyline, TCA: tricyclic antidepressants, SCD: sudden cardiac death, SCRs: spontaneous Ca^{2+} releases, SR: sarcoplasmic reticulum, RyR2: cardiac SR Ca^{2+} release channels, Casq2: cardiac calsequestrin

Molecular Pharmacology Fast Forward. Published on October 9, 2008 as DOI: 10.1124/mol.108.051490
This article has not been copyedited and formatted. The final version may differ from this version.

ABSTRACT

Patients taking amitriptyline (AMT) have an increased risk of sudden cardiac death, yet the mechanism for AMT's pro-arrhythmic effects remains incompletely understood. Here, we hypothesize that AMT activates cardiac ryanodine channels (RyR2) causing premature Ca^{2+} release from the sarcoplasmic reticulum (SR), a mechanism identified by genetic studies as a cause of ventricular arrhythmias and sudden cardiac death. To test this hypothesis, we measured AMT's effects on RyR2 channels from mice and sheep and on intact mouse cardiomyocytes loaded with the Ca^{2+} fluorescent indicator Fura-2AM. AMT induced trains of long channel openings (bursts) with 60-90% of normal conductance in RyR2 channels incorporated in lipid bilayers. The [AMT]-, voltage- and P_o-dependencies of burst frequency and duration indicated that AMT binds primarily to open RyR2 channels. AMT activated also RyR2 channels isolated from transgenic mice lacking cardiac calsequestrin. Reducing RyR2 P_o by increasing cytoplasmic [Mg^{2+}] significantly inhibited the AMT effect on RyR2 channels. Consistent with the single RyR2 channel data, AMT increased the rate of spontaneous Ca^{2+} releases and decreased the SR Ca^{2+} content in intact cardiomyocytes. Intracellular [AMT] were approximately 5-fold higher than extracellular [AMT], explaining AMT's higher potency in cardiomyocytes at clinically relevant concentrations (0.5-3 μmol/l) compared to its effect in lipid bilayers (5-10 μmol/l). Increasing extracellular [Mg^{2+}] attenuated the effect of AMT in intact myocytes. We conclude that the heretofore unrecognized activation of RyR2 channels and increased SR Ca^{2+} leak may contribute to AMT's pro-arrhythmic and cardiotoxic effects, which may be counteracted by interventions that reduce RyR2 channel open probability.

Molecular Pharmacology Fast Forward. Published on October 9, 2008 as DOI: 10.1124/mol.108.051490
This article has not been copyedited and formatted. The final version may differ from this version.

Clinical use of tricyclic antidepressants (TCA) is limited by their narrow therapeutic window, with significant cardiovascular toxicity (Thanacoody and Thomas, 2005) including sudden cardiac death (SCD) and myocardial depression (Pimentel and Trommer, 1994) reported in overdose cases. Even at therapeutic doses TCA, in particular AMT, increase the rate of SCD (Ray et al., 2004). Among the TCA, AMT is the agent most commonly associated with SCD (32%) in cases of acute overdose (Crouch et al., 2004). The therapeutic plasma concentration of AMT in humans is 0.3 µmol/l; acute toxicity starts at 1.5 µmol/l and is well established at 3 µmol/l (Hardman, 2001). Even though AMT acts on many cardiac membrane receptors, ion channels, transporters and intracellular proteins (Hardman, 2001) which may contribute to the AMT's toxic effect on the heart, the cause of AMT induced SCD remains incompletely understood (Heard et al., 2001). Specifically, QT prolongation is not commonly seen during chronic TCA therapy. Moreover, only 15% of overdose cases display QT prolongation (Vieweg and Wood, 2004), suggesting that other arrhythmia mechanisms are in play.

In cardiac muscle, sarcolemmal depolarization activates voltage-gated L-type Ca^{2+} channels in the T-tubules. The ensuing Ca^{2+} influx triggers Ca^{2+} release from the sarcoplasmic reticulum (SR) via ryanodine receptor Ca^{2+} release channels (RyR2), collectively referred to as 'excitation-contraction' (E-C) coupling. Sensitization of RyR2 channels causing spontaneous SR Ca^{2+} releases has been implicated as cause of delayed after-depolarization that can trigger ventricular arrhythmia and sudden cardiac death in both genetic and acquired arrhythmia syndromes in absence of QT prolongation (Knollmann and Roden, 2008).

Thus, we hypothesized that AMT activates RyR2 channel complex causing spontaneous SR Ca^{2+} release and SR Ca^{2+} store depletion in ventricular myocytes. This would constitute a novel molecular mechanism that could help explain the pro-arrhythmic effects and myocardial

Molecular Pharmacology Fast Forward. Published on October 9, 2008 as DOI: 10.1124/mol.108.051490
This article has not been copyedited and formatted. The final version may differ from this version.

depression associated with AMT use. To test this hypothesis, we examined the effects of AMT on the activity of single RyR2s in artificial lipid bilayers and on SR Ca^{2+} handling of isolated ventricular myocytes.

We found that AMT increases RyR2 channel activity in bilayers and causes spontaneous SR Ca^{2+}-release events and SR Ca^{2+} store depletion in intact myocytes at concentrations relevant in humans (0.5 to 3 μmol/l). The mechanism of this heretofore unrecognized AMT's action on SR Ca^{2+} handling is a direct activation of the RyR2 complex (i.e. the ryanodine receptor, and/or associated proteins excluding calsequestrin) by AMT. Mg^{2+} attenuated the effect of AMT, suggesting a possible mechanism for the beneficial effects of Mg^{2+} administration observed in patients with AMT-induced cardiotoxicity.

Molecular Pharmacology Fast Forward. Published on October 9, 2008 as DOI: 10.1124/mol.108.051490
This article has not been copyedited and formatted. The final version may differ from this version.

MATERIALS AND METHODS

Animal model: The use of animals in this study was in accordance with the guidelines set by the Animal Care and Use Committees of Georgetown and Vanderbilt Universities in USA, and University of Newcastle in Australia. A total of 37 age (2-4 months) and sex matched mice of C57/Bl6 background strain were used for all the experiments. In addition, 6 mice with gene-targeted ablation of cardiac calsequestrin (Casq2) as previously described (Knollmann et al., 2006) and one sheep was used for the study.

Preparation of SR Vesicles for lipid bilayer studies: All buffers contained the protease inhibitors: leupeptin (1 μg/ml), pepstatin A (1 μg/ml), benzamidine (1 mmol/l), and PMSF (0.5 mmol/l). Hearts were excised from mice anesthetized with inhaled mixture of 100% O_2 and isoflurane (Minrad Inc., Bethlehem, PA). After surgical level of anesthesia was confirmed by tail pinching, the heart was removed and the animal killed with exsanguination. Then the heart was rinsed in ice cold PBS before being snap frozen in liquid nitrogen. Hearts were stored at -80°C until required. 5-6 hearts were homogenized using a polytron homogeniser (30 s at high speed) in 5ml of ice cold homogenization buffer (in mmol/l); 10 imidazole, 0.5 DTT, 3 sodium azide, 290 sucrose, pH 6.9). The homogenate was centrifuged at 8,000 g for 20 min (Beckman Coulter TLA-110 @ 14,000 rpm). The supernatant was retrieved and spun at 417,000 g for 30 min (TLA-110 @ 100,000 rpm). This pellet was resuspended in 3ml of ice cold homogenization buffer also containing 0.65 mol/l KCl (KCl buffer) and incubated on ice for 30 min. The homogenate was spun at 3,000 g for 10 min (TLA-110 @ 9,000 rpm), supernatant recovered and spun at 417,000 g for 30 min. The pellet was resuspended in ~50 μl ice cold KCl buffer with 10 strokes of a teflon/glass homogenizer. Preparation was maintained at 4°C during use and stored at -80°C. SR

Molecular Pharmacology Fast Forward. Published on October 9, 2008 as DOI: 10.1124/mol.108.051490
This article has not been copyedited and formatted. The final version may differ from this version.

vesicles (containing RyR_2) were also obtained from sheep hearts and were reconstituted into artificial lipid bilayers as previously described (Laver et al., 1995).

Single channel measurements: Lipid bilayers were formed from phosphatidylethanolamine and phosphatidylcholine (8:2 wt/wt, Avanti Polar Lipids, Alabaster, AL) in n-decane, (50 mg/ml, ICN Biomedicals) across an aperture of 150–250 μm diameter in a Delrin cup. During SR-vesicle incorporation, the *cis* (cytoplasmic) solution contained (in mmol/l) 250 Cs^+ (230 $CsCH_3O_3S$, 20 CsCl), 1.0 $CaCl_2$ and 500 mannitol, while the *trans* (luminal) solution contained 50 Cs^+ (30 $CsCH_3O_3S$, 20 $CsCl_2$), and 0.1 $CaCl_2$. The osmotic gradient across the membrane and the Ca^{2+} in the *cis* solution aided vesicle fusion with the bilayer. After detection of RyR2 in the bilayer, 2 mmol/l ATP and BAPTA was added to the *cis* solution; bringing the free [Ca^{2+}] down to 0.1 μmol/l (4.5 mmol/l BAPTA) or 1 μmol/l (2 mmol/l BAPTA). Also, the [$CsCH_3O_3S$] in the *trans* solution was increased to 230 mmol/l (*i.e.* establishing 250 mmol/l Cs^+ in both *cis* and *trans* baths) by means of aliquot addition of 4 mol/l stock. AMT (Sigma) was added to the *cis* bath via aliquots of a 5 mmol/l stock in milliQ water. The cesium salts were obtained from Aldrich Chemical Company, mannitol was obtained from Ajax chemicals and $CaCl_2$ from BDH Chemicals. Solutions were pH-buffered with 10 mmol/l N-tris [Hydroxymethyl]methyl-2-aminoethanesulfonic acid (TES, ICN Biomedicals) and solutions were titrated to pH 7.4 using CsOH (optical grade, ICN Biomedicals).

During experiments the composition of the *cis* solution was altered either by addition of aliquots of stock solutions or by local perfusion of the bath near the bilayer. Local perfusion was done by flowing solution from a tube 300 μm ID and located within 100 μm of the bilayer. Flow rates of ~1 μl per second produced total solution exchange at the bilayer in <1 s (Laver and Curtis, 1996).

Molecular Pharmacology Fast Forward. Published on October 9, 2008 as DOI: 10.1124/mol.108.051490
This article has not been copyedited and formatted. The final version may differ from this version.

Bilayer potential was controlled using an Axopatch 200B amplifier (Axon Instruments). Electrical potentials are expressed using standard physiological convention (*i.e.*, cytoplasmic side relative to the luminal side at virtual ground). Single channel recordings were obtained using bilayer potential difference of +40 mV. The current signal was digitized at 5 kHz and low-pass filtered at 1 or 2 kHz with a Gaussian digital filter. Open probability (P_o) was measured by the 50% threshold detection method. Analysis was carried out using Channel2 software (P.W. Gage and M. Smith, Australian National University, Canberra). Unless otherwise stated, data is presented as mean ± SEM.

Dwell-time frequency histograms of channel openings were obtained from single channel recordings and were displayed as probabilities (counts/total number of events). These were plotted using the "log-bin" method suggested by Sigworth and Sine (Sigworth and Sine, 1987) which displays exponentials as peaked distributions centred about their exponential time constant.

Cardiomyocyte isolation: Single ventricular myocytes were isolated by a modified collagenase/protease method as previously described (Knollmann et al., 2006). All chemicals, unless otherwise specified were obtained from Sigma (St. Louis, MO). All the experiments were conducted in Tyrode's solution containing (in mmol/l): NaCl 134, KCl 5.4, $MgCl_2$ 1, glucose 10, and HEPES 10, pH adjusted to 7.4 with NaOH.

Ca^{2+} indicator loading and exposure to AMT: Myocytes were loaded with Fura-2 acetoxymethyl ester (Fura-2, AM; Invitrogen) as described previously (Knollmann et al., 2006). Myocytes were then incubated with AMT (Sigma, St. Louis, MO) (0, 0.5, 1, 3, 10, 300 µmol/l) in 5 mmol/l Ca^{2+} Tyrode's solution for 15 mins prior to the experiments and then studied in the presence of AMT for up to 2 hrs. Thus, on average, myocytes were exposed to the respective

Molecular Pharmacology Fast Forward. Published on October 9, 2008 as DOI: 10.1124/mol.108.051490
This article has not been copyedited and formatted. The final version may differ from this version.

AMT concentration for about 1 hr. Experiments were conducted in a parallel study design with respect to different drug concentrations, which were in turn random in sequence to minimize the effect of time when cells were studied after isolation. Data from multiple days were pooled for analysis. All experiments were conducted at room temperature (23 °C).

Ca^{2+} fluorescence measurements: Healthy quiescent Fura-2 loaded rod-shaped isolated ventricular myocytes were loaded in the experimental chamber, and superfused with Tyrode's solution containing 5 mmol/l Ca^{2+} and the desired AMT concentration. Intracellular diastolic Ca^{2+} fluorescence signal and myocyte sarcomere length were simultaneously measured using a dual beam excitation fluorescence photometry set-up (IonOptix, Milton, MA). Prior to measurement of store Ca^{2+} load, two recordings of Ca^{2+} fluorescence and cell length (10s long) were obtained from each myocyte to capture spontaneous SR Ca^{2+} release events. The SR Ca^{2+} content for each myocyte was estimated from the amplitude of the caffeine-induced Ca^{2+} transient during 4 second exposure to Tyrode's solution containing 10 mmol/l caffeine as described previously (Knollmann et al., 2006).

Analysis of spontaneous SR Ca^{2+} release events (SCRs): The spontaneous SR Ca^{2+} release events (SCRs) were recorded from individual myocytes exposed to increasing AMT concentration. A SCR was defined as any increase in Ca^{2+} fluorescence signal (F_{ratio}) of 0.1 ratiometric units (three times the average background noise) or more from the baseline diastolic signal other than when triggered by caffeine. All SCRs during a 40-second recording period from individual myocytes were counted and reported as an average number of events/second.

In a subset of experiments, SCRs were also recorded from myocytes exposed to 0 and 1 µmol/l AMT in Na^{+} and Ca^{2+} free extracellular solutions to prevent any confounding from trans-sarcolemmal Ca^{2+} fluxes. During these experiments the myocytes were first loaded in 5 mmol/l

Molecular Pharmacology Fast Forward. Published on October 9, 2008 as DOI: 10.1124/mol.108.051490
This article has not been copyedited and formatted. The final version may differ from this version.

Ca^{2+} Tyrode's solution to load the SR. The composition of the 0 Ca^{2+}, 0 Na^{+} Tyrode's solution was (in mmol/l): LiCl 134, KCl 5.4, $MgCl_2$ 1, EGTA 1, glucose 10, and HEPES 10, pH adjusted to 7.4 with LiOH.

Measurement of SR Ca^{2+} leak: SR Ca^{2+} leak was measured in myocytes exposed to 0 and 1 μmol/l AMT in 0Ca^{2+}, 0Na^{+} Tyrode's solution to eliminate trans-sarcolemmal Ca^{2+} fluxes (Shannon et al., 2002). After achieving steady-state the external solution was quickly changed to one containing 1 mmol/l tetracaine in Tyrode solution 0Ca^{2+}, 0Na^{+} for 20 seconds. Tetracaine blocks the RyR2 causing a drop in cellular Ca^{2+} fluorescence which represents shift of Ca^{2+} from the cytosol into the SR. The tetracaine-induced drop in diastolic Fura-2 fluorescence ratio was used as an estimate of SR Ca^{2+} leak as described previously (Shannon et al., 2002).

Measurement of AMT by ESI/LC/MS/MS: To determine optimal instrument parameters for measurement of AMT, 100 μmol/l AMT was infused into a Quantum TSQ triple quadrapole mass spectrometer operating in positive ion mode. Collision induced disassociation of the *m/z* 278 [M+H^{+}] ion for AMT produced ions of *m/z* 233 (-18eV), 202 (-56eV), 191 (-26 eV) and 91(-38 eV). A similar strategy was employed to determine the optimal product ions for the internal standard imipramine (IMP). Collision induced disassociation of the *m/z* 281 [M+H+] ion for IMP produced ions of *m/z* 208 (-30 eV), 193 (-48 eV), 86 (-14eV), and 58 (-56eV).

A standard curve was prepared using 25 μl of 10 μg/mL IMP (0.89 nmol) spiked into 100 μl samples of 0-300 μmol/l AMT. 875 μl of 3% NH_4OH was then added to each sample and 6 ml of n-hexanes added to extract AMT and IMP. The hexane (upper) layer was dried down and resuspended in 100 μl methanol. Samples were analyzed by LC/MS/MS using a C18 column (Magic Bullet C18 column 3A, Michrom BioResources, Auburn, CA, column volume ~25 μl) with the gradient programmed from 60% solvent A (0.5% NH_4OH in water) and 40% Solvent B

Molecular Pharmacology Fast Forward. Published on October 9, 2008 as DOI: 10.1124/mol.108.051490
This article has not been copyedited and formatted. The final version may differ from this version.

(0.5% NH_4OH in methanol) to 100% B over 2.5 minutes and then continuing at 100% B. Flow rate was 200 µl/min. Eluant was coupled directly to the mass spectrometer operated in selective reaction monitoring (SRM) positive ion mode monitoring the SRM transition *m/z* 278 → 191@-26eV for AMT and *m/z* 281 → 193@-48eV for IMP. Both compounds eluted at approximately 2.4 minutes. The standard curve gave a linear response (R^2=1.0) with moles AMT = $8.x10^{-10}$ x (ratio area of *m/z* 278 ion peak / area of *m/z* 281 ion peak)-$1.5x10^{-11}$.

Measurement of intracellular AMT concentration: Isolated myocytes were incubated with 0-300 µmol/l AMT in 5 mmol/l Ca^{2+} Tyrode's solution for 1 h. Since all the isolated myocytes experiments were done within 2 hours of AMT exposure, it was considered apt to measure intracellular AMT concentration at the mean time of 1 hour. Each concentration was performed in triplicate. After this incubation period, the cells were washed three times in 5 mmol/l Ca^{2+} Tyrode's solution to remove extracellular AMT. The pelleted myocytes were weighed and then resuspended in 1 ml of 3% NH_4OH. Twenty five µl of 10 µg/ml imipramine (IMP) was added as an internal standard and then 6 ml of n-hexanes added to extract the AMT and IMP. The hexane (upper) layer was dried down and resuspended in 100 µl methanol. AMT was quantified by LC/MS/MS as described above. The intracellular concentration of AMT was calculated as moles of AMT in the sample determined by LC/MS/MS divided by the pelleted cell volume of the sample using a density of 1 µl per 1 mg pellet weight.

Statistical Analysis: Experiments on SR Ca^{2+} release were done in random sequence with respect to AMT concentrations. Differences between groups were assessed using a one-way analysis of variance. If statistically significant differences were found, individual groups were compared with *Student's t*-test or by non-parametric tests as indicated in the text. Results were

Molecular Pharmacology Fast Forward. Published on October 9, 2008 as DOI: 10.1124/mol.108.051490
This article has not been copyedited and formatted. The final version may differ from this version.

considered statistically significant if the *p*-value was less than 0.05. Unless otherwise indicated, results are expressed as arithmetic means and standard error of mean.

Molecular Pharmacology Fast Forward. Published on October 9, 2008 as DOI: 10.1124/mol.108.051490
This article has not been copyedited and formatted. The final version may differ from this version.

RESULTS

AMT directly activates RyR2 channels in lipid bilayers:

First, we determined the effect of increasing cytoplasmic (*i.e. cis*) AMT concentration on native RyR2 channels isolated from sheep heart in the presence of *cis* 2 mmol/l ATP and 1 μmol/l Ca^{2+} (systolic [Ca^{2+}]) at a holding potential of 40 mV (Figure 1). Channels were responsive to ryanodine and ruthenium red, which identifies them as RyRs (Figure 1C). In the absence of AMT, sheep RyR2 had an open probability, P_o, of 0.31 ± 0.09, mean open time, τ_o, of 6.7 ± 1.0 ms and mean closed time, τ_c, of 14 ± 7 ms and peak current, I, of 18.4 ± 0.8 pA (n=5) (*e.g.* Figure 1A, top trace). Addition of AMT (10 μmol/l) caused intermittent bursts of extended channel openings (Figure 1A, underscored sections in traces 2-6) amid channel activity that was indistinguishable from control. Analysis of sections of channel activity between bursts in traces 2 & 3 gave P_o = 0.14 ± 0.04, τ_o = 4.0 ± 0.4 ms, τ_c = 25 ± 8 ms and I = 18.2 ± 0.7 pA (n=5). The AMT induced bursts exhibited markedly different conductance and gating properties to control activity (Figure 1B, see features labeled a-c). Amplitude histograms of channel events show that these bursts had two prominent conductance levels (Figure 2A, arrows) corresponding to 60% and 85% of the maximal conductance RyR2 in the absence of AMT. The 85% conductance level exhibited very brief channel closures (< 1 ms, Figure 1Ba) whereas during the 60% level channel closures were rare (Figure 1Bb). The channels also had periods of channel closures with brief openings (Figure 1Bc). The probability of these AMT-induced bursts increased from 0.2 to 0.8 over the concentration range 10 to 50 μmol/l (Figure 2B).

Figure 3 shows dwell-time histograms of channel openings (Figure 3A) and closures (Figure 3B) in the absence and presence of AMT. (All histograms could be fitted by the sum of two exponentials, fits not shown). The AMT induced bursts has very different open and closed

Molecular Pharmacology Fast Forward. Published on October 9, 2008 as DOI: 10.1124/mol.108.051490
This article has not been copyedited and formatted. The final version may differ from this version.

dwell-time distributions. The mean channel open time in AMT induced bursts was 37 ms which is 10-fold longer than during control activity (3.4 ms). Mean closed times during bursts were ~30x shorter than control (1.3 ms *vs* 35 ms, respectively). The dwell-time histograms obtained from channel activity in between the AMT induced bursts were indistinguishable from those obtained in the absence of AMT (*c.f.* ○ & ● in Figure 3). This is consistent with AMT induced bursts being associated with times when AMT is bound to the RyR and that during the inter-burst periods AMT is not bound.

Kinetics of AMT activation in RyR2 channels*:*

We inferred the kinetics of AMT binding by measuring the duration of the AMT induced opening bursts and the intervals between them in RyR2 channels. In the absence of AMT, RyR2 exhibited a well characterised modal gating phenomenon (Zahradnikova et al., 1999) in which channels would randomly fluctuate between periods of high and low P_o over periods of tens of seconds. An example of this can be seen in Figure 1A where P_o between AMT bursts transiently decreases during trace 3. We also noticed that the separation between AMT induced bursts was generally longer during periods of low RyR2 P_o suggesting that AMT binding requires that RyRs be open. To quantify this effect we measured the P_o of RyRs during each interburst period. We then correlated the reciprocal of each burst gap duration (*i.e.* burst frequency, F) with the P_o of the RyR2 during that gap (Figure 4A). This analysis shows that F and P_o are proportional over a wide range of P_o. In other words, long burst gaps are associated with low P_o. The linear correlation between F and P_o confirms that AMT induced bursts are primarily initiated during the open channel configuration. We derived the association rate of AMT, k_+, by fitting the correlation between F and P_o with the equation $F = P_o\, k_+$ (*c.f.* line and ● in Figure 4A). This

Molecular Pharmacology Fast Forward. Published on October 9, 2008 as DOI: 10.1124/mol.108.051490
This article has not been copyedited and formatted. The final version may differ from this version.

equation can be recast into the form $F_o = k_+$, where F_o is the reciprocal of the mean total open time between bursts. We also calculated the dissociation rate, k_-, which is equal to the reciprocal of mean burst duration provided that the duration of AMT induced bursts reflects the period that AMT is bound to the RyR. We note that the duration of AMT induced bursts were shorter following inter burst periods of RyR2 activity with relatively low mean open time (τ_o, Figure 4B) indicating a link between RyR2 closing rate in the absence of AMT and k_-.

Increasing AMT concentration up to 50 μmol/l caused a proportional increase in F_o but had no significant effect on the burst durations (Figure 4C and D). Once again, this is consistent with an AMT activation mechanism in which the bursts represent periods where AMT is bound to the RyR2 and that AMT binding occurs mainly while the channel is open. The association rate constant, α, is calculated from the [AMT]-dependence of F_o using the equation $\alpha = F_o/[\text{AMT}]$ ($F_o = k_+$). The dissociation rate constant, β, was equal to k_-. Linear, fits to the data in Figures 4C and D gives values for the rate constants of $\alpha = 0.27 \pm 0.025$ $(\mu\text{mol/l*s})^{-1}$ and $\beta = 0.3 \pm 0.2$ s^{-1} (+40 mV). We found that α was strongly voltage-dependent whereas β showed no significant dependence on voltage (Figure 4E & F, ●). We also measured the frequency and duration of AMT induced bursts in mouse wild-type (*Casq2*$^{+/+}$) RyR2 under the same conditions as we did for sheep RyRs and found that AMT binding kinetics were not significantly different between RyRs from mouse and sheep (*c.f.* □ & ● in Figure 4E and F).

We investigated the possibility of a luminal facing AMT site on the RyR2 by applying AMT to the luminal (*trans*) bath. We found that AMT induced bursts of channel openings with conductance levels identical to those induced by cytoplasmic AMT (*records not shown*). Moreover, the slopes of the voltage-dependencies of the rates for AMT association and dissociation were not significantly different for luminal and cytoplasmic AMT. The only

Molecular Pharmacology Fast Forward. Published on October 9, 2008 as DOI: 10.1124/mol.108.051490
This article has not been copyedited and formatted. The final version may differ from this version.

difference was that at a given voltage, the RyR2 was slightly less sensitive to luminal AMT (*i.e.* AMT had a lower association rate and higher dissociation rate from the luminal side, Figure 4E & F, ○).

Since luminal and cytoplasmic AMT had nearly identical effects on RyR2 activity it is likely that the same AMT binding site is accessible from both sides of the membrane. AMT partitions into the bilayer such that the hydrophobic portion of the molecules incorporates into the acyl chains of the lipids and the charged amino group resides among the polar heads groups (Deo et al., 2004). This study showed that the mole fraction of AMT in the bilayer is ~0.01 when its concentration in the bath was 10 μmol/l. Therefore we considered the possibility that AMT can adsorb to bilayers and/or permeate them prior to reaching its site of action. To test for this we measured the rate of reversal of the AMT effect after washout of the drug from the cytoplasmic bath. Compounds can be washed out of the bath within ~1 s as we show in Figure 5C. However, drugs that partition into the bilayer are slow to exchange with the aqueous phase and could be retained in the lipids for some time after they have been removed from the bath. Reversal of AMT activation of RyR2s was assessed by measuring RyR2 burst frequency (F_o) at different time points after perfusion was initiated (Figure 5A). RyR2s were initially exposed to 50 μmol/l AMT via aliquot addition to the cytoplasmic bath. When the bilayer and RyR2 were perfused with AMT-free solution so that AMT had been removed from the vicinity of the bilayer (see Methods) AMT-induced bursts continued to occur for several minutes. Figure 5B shows accumulated data obtained from several RyR2s exposed to 2-6 repeats of 2 min episodes of bath perfusion. Repeats were achieved by switching off the perfusion to allow AMT to gain access to the bilayer and RyR2. During perfusion F_o declined exponentially with a decay constant of 17 ± 4 s (equivalent to a 12 s half-time). This is considerably slower than the time course of AMT

Molecular Pharmacology Fast Forward. Published on October 9, 2008 as DOI: 10.1124/mol.108.051490
This article has not been copyedited and formatted. The final version may differ from this version.

washout from the aqueous phase (<1 s half-time) which indicates either 1) that AMT binds to the RyR2 from within the bilayer or 2) that the membrane lipids provide a reservoir of AMT to activate RyR2s. We argue for the latter possibility (see Discussion)

Since the binding of AMT depends on the open conformation of the RyR2, we examined the effect on AMT binding of cytoplasmic Ca^{2+} and Mg^{2+} which are known to modulate the P_o of RyR2. The effects of Ca^{2+} and Mg^{2+} on the duration and frequency of AMT induced bursts are summarised in Table 1. Reducing [Ca^{2+}] from 1 μmol/l to 0.1 μmol/l caused a 7-fold decrease in the AMT bursting rate ($F/(\mu$mol/l)) whereas the association rate to the open state ($F_o/(\mu$mol/l)) was not significantly affected. These results are in line with the effect of P_o on AMT binding shown in Figure 4A. Moreover, decreasing [Ca^{2+}] decreased burst duration in association with a decrease in τ_o similar to that seen in Figure 4B. A similar pattern occurred with Mg^{2+} where the addition of Mg^{2+} (220 μmol/l free Mg^{2+} in the presence of 0.1 μmol/l Ca^{2+}) to the cytoplasmic bath decreased RyR2 P_o and τ_o in conjunction with a decreased AMT bursting rate and duration. Once again, F_o was not significantly affected by Mg^{2+}. Thus it appears that AMT is more able to bind to, and modify RyR2 gating under conditions where the RyR2 are more active.

AMT activates RyR2 at low concentrations and inhibits them at high concentrations:

RyR2 activation and inhibition (sheep RyR2) was also seen in single channel recordings in the presence of 1 μmol/l Ca^{2+} (Figures 6A and B). At concentrations up to 200 μmol/l, AMT induced long lived substates in the channel record just as shown in Figures 1 & 5. However, at higher concentrations (500 and 1000 μmol/l), AMT caused brief channel closures that gave the recordings a flickery appearance. The inhibitory effect of AMT was similar at both +40 mV and -40 mV indicating that inhibition not voltage-dependent like the AMT activation process. These

Molecular Pharmacology Fast Forward. Published on October 9, 2008 as DOI: 10.1124/mol.108.051490
This article has not been copyedited and formatted. The final version may differ from this version.

data demonstrate that AMT has a high affinity activation site and a lower affinity inhibition site. The inhibitory action of AMT at such high concentrations was not studied in detail as it is unlikely to be important to the clinical action of this drug.

AMT does not require the presence of Casq2 to activate RyR2 channels:

Since AMT is known to bind to Casq2 (Park et al., 2005), and Casq2 prominently regulates RyR2 channel open probability (Gyorke et al., 2002), we investigated the possibility that Casq2 is the binding site responsible for the AMT induced channel opening we observe. Thus, we determined the effect of increasing cytoplasmic (*i.e. cis*) AMT concentration on RyR2 channels isolated from *Casq2*$^{+/+}$ and *Casq2*$^{-/-}$ mice in the presence of *cis* 2 mmol/l ATP and 0.1 μmol/l Ca^{2+} (diastolic [Ca^{2+}]) at a holding potential of 40 mV (Figure 7A and B). RyR2 from *Casq2*$^{+/+}$ mouse heart had an open probability, P_o, of 0.042 ± 0.018, mean open time, τ_o, of 1.9 ± 0.5 ms and mean closed time, τ_c, of 210 ± 120 ms (n=6). In the *Casq2*$^{-/-}$ RyR2 the mean P_o was 0.0180 ± 0.0086, mean open time, τ_o, of 3.5 ± 1.5 ms and mean closed time, τ_c, of 633 ± 320 ms (n=7). Even though generally lower, the P_o of RyR2 from *Casq2*$^{-/-}$ hearts was not significantly different than those derived from *Casq2*$^{+/+}$ mouse (p = 0.11). The RyR2 maximum current was also not significantly different between *Casq2*$^{+/+}$ (16.1 ± 0.4 pA at +40 mV) and *Casq2*$^{-/-}$ mice (16.2 ± 0.5 pA at +40 mV).

AMT concentrations of 5-10 μmol/l produced its typical bursting phenomenon in RyR2 channels, regardless of whether Casq2 was present or not (Figure 7A and B). AMT induced bursts had extended openings with two prominent conductance levels corresponding to 70 and 90% of the maximal conductance RyR2 in the absence of AMT. In RyR2 from both *Casq2*$^{+/+}$ and *Casq2*$^{-/-}$ mice, AMT increased P_o by 4-6 fold at 5-10 μmol/l (Figure 7C). This activation was

Molecular Pharmacology Fast Forward. Published on October 9, 2008 as DOI: 10.1124/mol.108.051490
This article has not been copyedited and formatted. The final version may differ from this version.

mediated mainly by an increase in τ_o. Thus, AMT binding to Casq2 is not necessary for AMT activation of RyR2 channels.

AMT reduces SR Ca^{2+} content in intact myocytes:

To assess the consequences of AMT's effects on RyR2 channels in intact myocytes, we loaded isolated mouse ventricular myocytes with the Ca^{2+} fluorescent indicator Fura-2 AM and exposed the myocytes to increasing concentrations of AMT. High extracellular Ca^{2+} (5 mmol/l) was used to maximally load the SR with Ca^{2+} and thereby enhance our ability to detect any effects of AMT on SR Ca^{2+} handling. SR Ca^{2+} content was estimated by rapid exposure to caffeine (10 mmol/l) and the amplitude of the caffeine-induced Ca^{2+} transient was taken as a measure of SR Ca^{2+} content (Figure 8A). AMT reduced SR Ca^{2+} content in a concentration dependent manner suggesting that its activation of RyR2 channels depletes SR Ca^{2+} stores (Figure 8A and B).

AMT causes spontaneous SR Ca^{2+} release:

To further probe the mechanism of reduction in SR Ca^{2+} content induced by AMT, we analyzed spontaneous SR Ca^{2+} release events (SCRs) in intact mouse ventricular myocytes exposed to increasing AMT concentrations (Figure 9A). We have previously shown that SCRs are caused by increased Ca^{2+} leak from the SR and are associated with ventricular arrhythmias (Chopra et al., 2007; Knollmann et al., 2006).

The rates of SCRs increased significantly from control condition (0 μmol/l AMT) to 0.5 and 1 μmol/l AMT in a concentration-dependent fashion, with a 4-fold increase observed at 1 μmol/l AMT in myocytes (Figure 9B). The increase in SCRs probably contributes to reduction of

Molecular Pharmacology Fast Forward. Published on October 9, 2008 as DOI: 10.1124/mol.108.051490
This article has not been copyedited and formatted. The final version may differ from this version.

SR Ca^{2+} content at concentrations <3 µmol/l (Figure 8B). However, at high concentrations of AMT (>3 µmol/l) the rate of SCRs started to decline (Figure 9B), probably due to concentration-dependent decline in SR Ca^{2+} content (Figure 8B). Consistent with the SR Ca depletion and increased rate of SCRs, AMT at 1, 3 and 10 µmol/l also significantly increased diastolic Ca^{2+} (Average diastolic Fura2 fluorescence ratio at respective AMT concentration: 0 µmol/l: 1.07+/-0.02, 1 µmol/l: 1.22+/-0.03, 3 µmol/l: 1.14+/-0.03, 10 µmol/l: 1.25 +/-0.03, $p<0.01$ compared with 0 µmol/l). AMT concentrations > 10 µmol/l had no significant effect on diastolic Ca^{2+}, probably as the result of their profound SR Ca^{2+} depletion during the incubation period.

To probe the relationship of SCRs and SR Ca^{2+} content upon exposure to AMT, we next examined the effect of 1 µmol/l AMT in myocytes with different SR Ca^{2+} content. As expected from the regulation of RyR2 by SR luminal Ca^{2+} (Gyorke et al., 2002), the rate of SCRs increased with increasing SR Ca^{2+} load. AMT significantly increased the rate of SCRs at all SR Ca^{2+} contents examined (Figure 9C).

Rapid depletion of SR Ca^{2+} content with caffeine (10 mmol/l) abolished SCRs until the SR refilled (*data not shown*), suggesting the SR as the source of SCRs. Furthermore, the SCRs were reminiscent of a low-dose (500 µmol/l) caffeine effect on RyR2 channels (Venetucci et al., 2007). Nevertheless, to exclude any possible contribution of trans-sarcolemmal Ca^{2+} influx triggering SCRs, we next quantified SCRs rates in myocytes bathed in Na^{+} and Ca^{2+} free extracellular solutions. The rate of SCRs remained significantly higher in the myocytes exposed to 1 µmol/l AMT (Figure 10A and B), which demonstrates that the SCRs were the result of intracellular SR Ca^{2+} release and not caused by Ca^{2+} influx across the sarcolemma. Since the Na-Ca exchanger is blocked under these experimental conditions, the amplitude of SCRs was higher compared with experiments in Na^{+} containing bath solutions (compare Figure 9A and Figure

Molecular Pharmacology Fast Forward. Published on October 9, 2008 as DOI: 10.1124/mol.108.051490
This article has not been copyedited and formatted. The final version may differ from this version.

10A). Taken together, these data suggest that AMT activation of RyR2 channels causes the increased rate of SCRs in intact myocytes. Ca^{2+} or Na^{+} influx into the myocyte is not required for the effect of AMT.

AMT increases SR Ca^{2+} leak in intact myocytes:

Another predicted consequence of increasing RyR2 channel open probability in intact myocytes is an increase in SR Ca^{2+} leak, which has been associated with SCRs and triggered arrhythmias (Knollmann et al., 2006). Therefore, we next estimated SR Ca^{2+} leak in isolated ventricular myocytes exposed to 1 and 0 µmol/l AMT using the RyR2 channel inhibitor tetracaine (Shannon et al., 2002). Consistent with our hypothesis, we found a significantly increased SR Ca^{2+} leak in myocytes exposed to 1 µmol/l compared to 0 µmol/l AMT (Figure 10A and C). Thus, AMT concentrations of 1 µmol/l are sufficient to activate RyR2 channels and cause spontaneous SR Ca^{2+} release in intact myocytes.

AMT accumulates in myocytes:

Compared with its effects on single channels in lipid bilayer, AMT caused an effect in intact myocytes at lower concentrations (0.5 µmol/l vs 5 µmol/l, compare Fig. 7 and 8). We next determined the intracellular concentration of AMT in the myocytes by mass spectrometry after one hour exposure to extracellular AMT. Intracellular AMT concentrations were at least 5-fold higher than extracellular concentrations at all (0.5-300 µmol/l) AMT concentrations examined (Figure 11). Thus, intracellular AMT accumulation may contribute to the higher potency of AMT in intact myocytes.

Molecular Pharmacology Fast Forward. Published on October 9, 2008 as DOI: 10.1124/mol.108.051490
This article has not been copyedited and formatted. The final version may differ from this version.

Mg^{2+} restores SR Ca^{2+} content and decreases rates of SCRs in AMT-exposed myocytes:

Our bilayer data show that AMT binds preferentially to open RyR2 channels and that reducing RyR2 channel P_o by increasing cytoplasmic Mg^{2+} concentration decreases AMT activation of RyR2 channels (Table 1). Thus, we next tested whether Mg^{2+} can also attenuate AMT-induced effects on SR Ca^{2+} handling in intact myocytes. Myocytes were incubated for 60 minutes in solutions containing either 1 mmol/l or 5 mmol/l Mg^{2+} and then exposed to different AMT concentrations. Pretreatment with high Mg^{2+} increased SR Ca^{2+} content in myocytes regardless of whether AMT was present or not (Figure 12A), consistent with the stabilizing effect of Mg^{2+} on the RyR2 complex (Laver et al., 1997). Interestingly, high Mg^{2+} specifically prevented the AMT-induced increase in SCRs in myocytes (Figure 12B). Thus, use of Mg^{2+} could be a therapeutic approach in AMT cardiotoxicity by counteracting AMT's actions on the RyR2 channel complex.

Molecular Pharmacology Fast Forward. Published on October 9, 2008 as DOI: 10.1124/mol.108.051490
This article has not been copyedited and formatted. The final version may differ from this version.

DISCUSSION

Our data demonstrate a novel mechanism of action for AMT: AMT activates the RyR2 SR Ca^{2+} release complex. Cardiac calsequestrin, also associated with the RyR2 complex and a putative AMT binding site, is not required for AMT action. AMT binds preferentially to open RyR2 channels, locking them in a sub-conductance state. The activation of RyR2 channels appears to be the main mechanism by which AMT causes SR Ca^{2+} leak, generates spontaneous SR Ca^{2+} release and eventually depletes SR Ca^{2+} stores. Given that AMT activates the RyR2 SR Ca^{2+} release complex at concentrations that are commonly observed in patients taking AMT (Hardman, 2001), the AMT action on RyR2 channels may contribute to the cardiotoxicity of AMT in patients.

Mechanisms of AMT activation of RyR2 channels

The action of AMT on cardiac RyR2s has marked similarities to that of ryanoids such as ryanodine, ryanodol (Tanna et al., 2000) and 21-amino-9α-hydroxy-ryanodine (Tanna et al., 1998). Both AMT and the ryanoids only appear to bind to the channel in its open state and induce long lasting channel sub-conductance states. Moreover, AMT and ryanodine activate RyR2s at low concentrations while at concentrations above 100 μmol/l both molecules inhibit them (Buck et al., 1992). The ryanodine binding site has been located in the 76 kDa region of RyR1 between amino acid position 4475 and the C-terminus, a region which contains the putative channel pore (Callaway et al., 1994). The voltage-dependence of AMT binding also suggests a binding site in the trans-membrane C-terminus of the RyR. However, in the case of ryanodols, comparative molecular field analysis of their effect on channel conductance suggests that they bind away from the ion conducting pathway; probably in the channel vestibule (Welch et al., 1994). Interestingly,

Molecular Pharmacology Fast Forward. Published on October 9, 2008 as DOI: 10.1124/mol.108.051490
This article has not been copyedited and formatted. The final version may differ from this version.

X-ray crystal structure of the leucine transporter from *Aquifex aeolicus* has revealed a TCA binding site at the inner end of its extra cellular cavity (Zhou et al., 2007). This site is located within the membrane and binding of the TCA constrains the trans-membrane α-helix, TM1, to prevent leucine release into the cytoplasm.

The mechanism for the voltage-dependence of AMT binding is not yet clear. Since AMT is cationic in aqueous solutions (pKa=9.2 (Deo et al., 2004)), it is possible that the voltage-dependence stems from the voltage difference between the binding site and the luminal and cytoplasmic baths. However, according to the Woodhull model (Woodhull, 1973), RyR2 activation by luminal and cytoplasmic AMT should have opposite voltage-dependencies because the trans-membrane electric field will have opposite effects on the binding of AMT molecules originating from luminal and cytoplasmic baths. This prediction does not tally with our data in Figure 4E which shows that the slope of the voltage-dependencies of cytoplasmic and luminal AMT binding are identical. A more likely explanation is that AMT binding is determined by the voltage-dependent properties of the AMT binding site and/or AMT molecule such as has been proposed for ryanodine related compounds (Tanna et al., 2000). Furthermore, the fact that cytoplasmic and luminal AMT induce identical RyR2 gating patterns with identical voltage-dependencies indicates that the same site/sites can be accessed by AMT molecules from both sides of the membrane. This hypothesis is consistent with the known partitioning of AMT into lipid bilayers (Deo et al., 2004) and the slow reversibility of AMT activation seen in Figure 5.

Role of AMT action on the RyR2 SR Ca^{2+} release complex in myocardial contractile dysfunction and sudden cardiac death

Molecular Pharmacology Fast Forward. Published on October 9, 2008 as DOI: 10.1124/mol.108.051490
This article has not been copyedited and formatted. The final version may differ from this version.

To date, both the pro-arrhythmic risk and myocardial contractile depression observed in AMT overdose have been primarily attributed to Na^+ channel block (Pimentel and Trommer, 1994; Thanacoody and Thomas, 2005). Nonetheless, mechanisms by which AMT decreases contractile function remain incompletely understood (Pimentel and Trommer, 1994). Factors other than sodium channel block have been implicated for direct myocardial contractile impairment in overdose situations (Knudsen and Abrahamsson, 1994). Thus, the heretofore unrecognized activating effect of AMT on the RyR2 complex may explain several aspects of AMT-induced cardiotoxicity: AMT causes spontaneous SR Ca^{2+}-release events (Figure 9), which are known to cause delayed after-depolarizations and predispose to ventricular arrhythmias and sudden cardiac death (Wit and Rosen, 1983). Thus, the effect of AMT is akin to that of RyR2 and Casq2 mutations causing spontaneous SR Ca^{2+}-release events and ventricular arrhythmia in mice and humans (Knollmann and Roden, 2008). Furthermore, the SR Ca^{2+} depletion observed at AMT concentration as low as 500 nmol/l in intact myocytes (Figure 8A and B) may cause myocardial contractile depression in overdose situations. AMT also inhibits the SR Ca^{2+} ATPase (SERCA) with a K_d of ~100 µmol/l (Kim et al., 2005). SERCA inhibition could contribute to the profound SR Ca^{2+} depletion seen with very high concentrations of AMT (Figure 8). It is also possible that AMT inhibits membrane proteins like L-type Ca^{2+} channels and Na/Ca exchanger at higher concentrations that would also deplete intracellular Ca^{2+}. However, these mechanisms are less likely relevant *in vivo* given that AMT concentrations in human plasma are ≤ 3 µmol/l.

The activating effect of AMT on the RyR2 complex may not be a 'class effect' in contrast to the Na^+ channel blockade seen with the TCAs. In a similar study, Watts *et al* found no effect of imipramine (a related TCA) on the caffeine-induced Ca^{2+} transients at 30 µmol/l concentration (Watts et al., 1998). This hypothesis has to be tested in future studies

Molecular Pharmacology Fast Forward. Published on October 9, 2008 as DOI: 10.1124/mol.108.051490
This article has not been copyedited and formatted. The final version may differ from this version.

RyR2 channel dysfunction is emerging as a paradigm for both genetic and acquired human diseases (Knollmann and Roden, 2008). While the intracellular RyR2 complex may not seem an obvious target for drug-related adverse effects; many drugs such as TCAs penetrate and accumulate inside myocytes (Walter and Gutknecht, 1986). Consistent with these reports, we demonstrate a five-fold increase of intracellular compared to extracellular AMT concentrations. Analogous to drug-acquired channelopathies such as K^+ channel blockade causing QTc prolongation and *torsades de pointe*, AMT's activation of the RyR2 complex may serve as a paradigm for drug related cardiotoxicity and should be considered whenever drug toxicity involves cardiomyopathy and ventricular arrhythmias without overt QTc prolongation.

RyR2 channel complex as a therapeutic target in AMT cardiotoxicity

The RyR2 channel complex may represent a target to prevent or treat AMT-induced cardiotoxicity. We show that Mg^{2+} blocks the direct activating effect of AMT on the RyR2 complex in both bilayers and intact myocytes. Mg^{2+} is known to inhibit the RyR2 channel by at least 2 different mechanisms (Laver et al., 1997). Since AMT binds to RyR2 channel in open state, presence of high Mg^{2+} can be predicted to attenuate the effect of AMT on the RyR2 complex. Consistent with this idea, we show that high Mg^{2+} prevented the AMT induced spontaneous Ca^{2+} release events in intact myocytes (Figure 12), which suggests that the effect of Mg^{2+} may be relevant in the intact cardiac muscle. This mechanism may partly explain the therapeutic efficacy of Mg^{2+} in the treatment of AMT cardiotoxicity in both humans (Citak et al., 2002) and rats (Knudsen and Abrahamsson, 1994).

Conclusion

Molecular Pharmacology Fast Forward. Published on October 9, 2008 as DOI: 10.1124/mol.108.051490
This article has not been copyedited and formatted. The final version may differ from this version.

AMT activates SR Ca^{2+} release by acting on the RyR2 channel itself, or associated proteins that are known to influence Ca^{2+} release. Also its action may be counteracted by increasing Mg^{2+}. Taken together, our results identify a novel mechanism of AMT action and suggest a potential therapeutic approach for the treatment of AMT-induced cardiotoxicity.

Molecular Pharmacology Fast Forward. Published on October 9, 2008 as DOI: 10.1124/mol.108.051490
This article has not been copyedited and formatted. The final version may differ from this version.

ACKNOWLEDGEMENTS

The authors wish to express their gratitude to Karl Pfeifer, National Institutes of Health, for his invaluable help generating the Casq2 mouse model, and Katherine Bradley and Paul Johnson for assisting with the bilayer experiments.

Molecular Pharmacology Fast Forward. Published on October 9, 2008 as DOI: 10.1124/mol.108.051490
This article has not been copyedited and formatted. The final version may differ from this version.

REFERENCES

Buck E, Zimanyi I, Abramson JJ and Pessah IN (1992) Ryanodine stabilizes multiple conformational states of the skeletal muscle calcium release channel. *J Biol Chem* **267**(33):23560-23567.

Callaway C, Seryshev A, Wang JP, Slavik KJ, Needleman DH, Cantu C, 3rd, Wu Y, Jayaraman T, Marks AR and Hamilton SL (1994) Localization of the high and low affinity [3H]ryanodine binding sites on the skeletal muscle Ca2+ release channel. *J Biol Chem* **269**(22):15876-15884.

Chopra N, Kannankeril PJ, Yang T, Hlaing T, Holinstat I, Ettensohn K, Pfeifer K, Akin B, Jones LR, Franzini-Armstrong C and Knollmann BC (2007) Modest reductions of cardiac calsequestrin increase sarcoplasmic reticulum Ca2+ leak independent of luminal Ca2+ and trigger ventricular arrhythmias in mice. *Circ Res* **101**(6):617-626.

Citak A, Soysal DD, Ucsel R, Karabocuoglu M and Uzel N (2002) Efficacy of long duration resuscitation and magnesium sulphate treatment in amitriptyline poisoning. *Eur J Emerg Med* **9**(1):63-66.

Crouch BI, Caravati EM, Mitchell A and Martin AC (2004) Poisoning in older adults: a 5-year experience of US poison control centers. *Ann Pharmacother* **38**(12):2005-2011.

Deo N, Somasundaran T and Somasundaran P (2004) Solution properties of amitriptyline and its partitioning into lipid bilayers. *Colloids Surf B Biointerfaces* **34**(3):155-159.

Gyorke S, Gyorke I, Lukyanenko V, Terentyev D, Viatchenko-Karpinski S and Wiesner TF (2002) Regulation of sarcoplasmic reticulum calcium release by luminal calcium in cardiac muscle. *Front Biosci* **7**:d1454-1463.

Hardman JG, Limbird, L. E. (2001) *Goodman and Gilman's The Pharmacological Basis of Therapeuics*. The McGraw-Hill companies, Inc., USA.

Heard K, Cain BS, Dart RC and Cairns CB (2001) Tricyclic antidepressants directly depress human myocardial mechanical function independent of effects on the conduction system. *Acad Emerg Med* **8**(12):1122-1127.

Kim E, Tam M, Siems WF and Kang C (2005) Effects of drugs with muscle-related side effects and affinity for calsequestrin on the calcium regulatory function of sarcoplasmic reticulum microsomes. *Mol Pharmacol* **68**(6):1708-1715.

Knollmann BC, Chopra N, Hlaing T, Akin B, Yang T, Ettensohn K, Knollmann BE, Horton KD, Weissman NJ, Holinstat I, Zhang W, Roden DM, Jones LR, Franzini-Armstrong C and Pfeifer K (2006) Casq2 deletion causes sarcoplasmic reticulum volume increase, premature Ca release, and catecholaminergic polymorphic ventricular tachycardia. *J Clin Invest* **116**(9):2510-2520.

Knollmann BC and Roden DM (2008) A genetic framework for improving arrhythmia therapy. *Nature* **451**(7181):929-936.

Knudsen K and Abrahamsson J (1994) Effects of epinephrine, norepinephrine, magnesium sulfate, and milrinone on survival and the occurrence of arrhythmias in amitriptyline poisoning in the rat. *Crit Care Med* **22**(11):1851-1855.

Laver DR, Baynes TM and Dulhunty AF (1997) Magnesium inhibition of ryanodine-receptor calcium channels: evidence for two independent mechanisms. *J Membr Biol* **156**(3):213-229.

Laver DR and Curtis BA (1996) Response of ryanodine receptor channels to Ca2+ steps produced by rapid solution exchange. *Biophys J* **71**(2):732-741.

Laver DR, Roden LD, Ahern GP, Eager KR, Junankar PR and Dulhunty AF (1995) Cytoplasmic Ca2+ inhibits the ryanodine receptor from cardiac muscle. *J Membr Biol* **147**(1):7-22.

Park IY, Kim EJ, Park H, Fields K, Dunker AK and Kang C (2005) Interaction between cardiac calsequestrin and drugs with known cardiotoxicity. *Mol Pharmacol* **67**(1):97-104.

Pimentel L and Trommer L (1994) Cyclic antidepressant overdoses. A review. *Emerg Med Clin North Am* **12**(2):533-547.

Ray WA, Meredith S, Thapa PB, Hall K and Murray KT (2004) Cyclic antidepressants and the risk of sudden cardiac death. *Clin Pharmacol Ther* **75**(3):234-241.

Shannon TR, Ginsburg KS and Bers DM (2002) Quantitative assessment of the SR Ca2+ leak-load relationship. *Circ Res* **91**(7):594-600.

Sigworth FJ and Sine SM (1987) Data transformations for improved display and fitting of single-channel dwell time histograms. *Biophys J* **52**(6):1047-1054.

Tanna B, Welch W, Ruest L, Sutko JL and Williams AJ (1998) Interactions of a reversible ryanoid (21-amino-9alpha-hydroxy-ryanodine) with single sheep cardiac ryanodine receptor channels. *J Gen Physiol* **112**(1):55-69.

Tanna B, Welch W, Ruest L, Sutko JL and Williams AJ (2000) The interaction of a neutral ryanoid with the ryanodine receptor channel provides insights into the mechanisms by which ryanoid binding is modulated by voltage. *J Gen Physiol* **116**(1):1-9.

Thanacoody HK and Thomas SH (2005) Tricyclic antidepressant poisoning: cardiovascular toxicity. *Toxicol Rev* **24**(3):205-214.

Venetucci LA, Trafford AW and Eisner DA (2007) Increasing ryanodine receptor open probability alone does not produce arrhythmogenic calcium waves: threshold sarcoplasmic reticulum calcium content is required. *Circ Res* **100**(1):105-111.

Vieweg WV and Wood MA (2004) Tricyclic antidepressants, QT interval prolongation, and torsade de pointes. *Psychosomatics* **45**(5):371-377.

Walter A and Gutknecht J (1986) Permeability of small nonelectrolytes through lipid bilayer membranes. *J Membr Biol* **90**(3):207-217.

Watts JA, Yates KM, Badar SK, Marcengill MB and Kline JA (1998) Mechanisms of Ca2+ antagonism in imipramine-induced toxicity of isolated adult rat cardiomyocytes. *Toxicol Appl Pharmacol* **153**(1):95-101.

Welch W, Ahmad S, Airey JA, Gerzon K, Humerickhouse RA, Besch HR, Jr., Ruest L, Deslongchamps P and Sutko JL (1994) Structural determinants of high-affinity binding of ryanoids to the vertebrate skeletal muscle ryanodine receptor: a comparative molecular field analysis. *Biochemistry* **33**(20):6074-6085.

Wit AL and Rosen MR (1983) Pathophysiologic mechanisms of cardiac arrhythmias. *Am Heart J* **106**(4 Pt 2):798-811.

Woodhull AM (1973) Ionic blockage of sodium channels in nerve. *J Gen Physiol* **61**(6):687-708.

Zahradnikova A, Dura M and Gyorke S (1999) Modal gating transitions in cardiac ryanodine receptors during increases of Ca2+ concentration produced by photolysis of caged Ca2+. *Pflugers Arch* **438**(3):283-288.

Zhou Z, Zhen J, Karpowich NK, Goetz RM, Law CJ, Reith ME and Wang DN (2007) LeuT-desipramine structure reveals how antidepressants block neurotransmitter reuptake. Science 317(5843):1390-1393.

Molecular Pharmacology Fast Forward. Published on October 9, 2008 as DOI: 10.1124/mol.108.051490
This article has not been copyedited and formatted. The final version may differ from this version.

FOOTNOTES

This work was supported in part by the National Institutes of Health grants HL88635 and HL71670 (to BCK), by the American Heart Association Established Investigator Award 0840071N (to BCK), by the Australian Research Council grant DP0557780 (to DRL), by an infrastructure grant from NSW Health through Hunter Medical Research Institute (DRL) and by a Senior Brawn Fellowship from the University of Newcastle (to DRL).

Part of this work has been presented at 2007 AHA annual scientific meeting (Chopra, N, Laver, D, Watanabe, H, Menon, U, Stein, CM, Knollmann, BC. Amitriptyline activates cardiac ryanodine receptors independently of its action on cardiac calsequestrin – Role for amitriptyline linked sudden cardiac death. Circulation 116(16):II-84, 2007) and 2008 Biophysics society annual scientific meeting (Laver, D, Chopra, N, Knollmann, BC. Mechanisms for Amitriptyline Activation of Cardiac RyRs and SR Ca^{2+} Release. Biophysical Journal 94:2120, 2008).

To whom reprint requests should be addressed: Björn C. Knollmann, M.D., Ph.D., Associate Professor of Medicine and Pharmacology, Oates Institute for Experimental Therapeutics, Division of Clinical Pharmacology, Vanderbilt University Medical Center, 1265 Medical Research Building IV, Nashville, TN 37232-0575. Office: (615) 343-6493, fax: (615) 343-4522, e-mail: bjorn.knollmann@vanderbilt.edu

[1]First two authors contributed equally to this study.

Molecular Pharmacology Fast Forward. Published on October 9, 2008 as DOI: 10.1124/mol.108.051490
This article has not been copyedited and formatted. The final version may differ from this version.

Legends for Figures

Figure 1. AMT activates cardiac RyR2s isolated from sheep. (A) A single channel recording of RyR2 from sheep heart representative of 5 experiments obtained at +40 mV (1 kHz filter). Dashed lines indicate the current baseline. The *cis* bath contained 2 mmol/l ATP and 1 μmol/l free Ca^{2+} (2 mmol/l BAPTA + 1 mmol/l $CaCl_2$). The top trace shows channel activity in the absence of AMT. The lower traces show continuous recordings of the same channel after the addition of 10 μmol/l AMT. AMT induces bursts of channel activity (underscored by bars) separated by control-like channel activity. **(B)** A section of recording from the second trace in A(●↔●) shown on the expanded time scale (2 kHz filter). The vertical arrow marks the time when the RyR switches between control-like activity and an AMT induced burst. Horizontal arrows mark two prominent subconductance states present in AMT induce burst activity. **(C)** The AMT induced channel responds to cytoplasmic ryanodine and ruthenium red as expected for a RyR. Top trace shows the addition of ryanodine to a channel that exhibits AMT induced bursts (a). Shortly after ryanodine addition (note the stirring noise) the channel enters a substate (b) that is characteristic of ryanodine binding to the RyR. The bottom trace shows the addition of ruthenium red to the same ryanodine modified channel. Ruthenium red causes a flicker block which progresses into total inhibition of the channel after 10s.

Figure 2. Properties of AMT-induced bursts under conditions described in Figure 1. **(A)** Current amplitude distributions from single channel recordings in Figure 1A. Control recording taken from trace 1 and those in the presence of AMT from traces 2-6. AMT induced channel substates are indicated by peaks in the distribution (arrows). **(B)** The dependence of AMT-induced bursts

Molecular Pharmacology Fast Forward. Published on October 9, 2008 as DOI: 10.1124/mol.108.051490
This article has not been copyedited and formatted. The final version may differ from this version.

probability on concentration. Burst probability was calculated from the ratio of the total burst duration and the record length.

Figure 3. Open **(A)** and closed **(B)** dwell-time histograms from single channel recordings in Figure 1A. The data are plotted using the log-bin method (Sigworth and Sine, 1987) using log-bins with 7 per decade (2 kHz filter). (●) Dwell-times from control activity in the top trace of Figure 1A. (○) Dwell-times from control-like activity between AMT induced bursts in the second and third traces in Figure 1A. (curves) Dwell-times from all the AMT induced bursts shown in Figure 1A.

Figure 4. The properties of AMT induced openings (bursts) in cardiac RyR2s from sheep and mouse heart. The effects on sheep RyR2 of AMT in the *cis* (●) or *trans* (○) baths and *cis* AMT on mouse RyRs (*Casq2*$^{+/+}$,□) were measured in the presence of 2 mmol/l ATP and 1 μmol/l free Ca^{2+} (2 mmol/l BAPTA + 1 mmol/l $CaCl_2$) and at +40 mV (unless specified otherwise). **(A)** The correlation between burst frequency (*F*= reciprocal of the inter burst interval) on the open probability of the channel during the burst interval in the presence of 10 μmol/l AMT. The data are grouped (n= 4-18) from 50 inter burst intervals from 6 sheep RyR2s and from 12 inter burst intervals from 2 mouse RyR2s. (Channels under control conditions normally exhibit fluctuations in P_o, τ_o and τ_c under steady experimental conditions, see text for details). The line depicts the least squares fit of the equation $F = P_o\, k_+$ to ● with $k_+ = 1.7 \pm 0.4\ s^{-1}$ (the intercept at $P_o = 1$). **(B)** The correlation between burst duration and τ_o during the preceding burst interval derived from the same single channel data as used for (A). **(C-D)** Derivation of rate constants for

Molecular Pharmacology Fast Forward. Published on October 9, 2008 as DOI: 10.1124/mol.108.051490
This article has not been copyedited and formatted. The final version may differ from this version.

AMT association, α, and dissociation, β, from the concentration-dependencies of F_o (the reciprocal of the total open period between bursts) (C) and burst duration (D). The data points show the mean and SEM of 3 - 6 measurements. (C-line) The fit of $\alpha = F_o/[AMT]$ to the data where the slope = $\alpha = 0.27 \pm 0.025$ $(\mu mol/l*s)^{-1}$ and the intercept = 0. (D-line) Linear fit to the data with slope=-0.003 ± 0.06 $(\mu mol/l)^{-1}s$, intercept = $\beta^{-1} = 3.2 \pm 2.0$ s. (**E, F**) Voltage-dependencies of α and β from luminal (*trans*) and cytoplasmic (*cis*) sides of the membrane. In E and F, the data points show the mean and SEM of 3-8 measurements and linear fits to the sheep log-data are shown as solid lines. Line parameters are: E- (solid) slope=0.017 ± 0.003 mV^{-1}, intercept = -4.2 ± 0.1; E- (dashed) slope=0.017 ± 0.005 mV^{-1}, intercept = -4.75 ± 0.16; F- (solid) slope=0.002 ± 0.004 mV^{-1}, intercept = -4.4 ± 0.2; F- (dashed) slope=0.003 ± 0.003 mV^{-1}, intercept = -0.4 ± 0.1.

Figure 5. Slow reversal of AMT activation upon washout. (A) A continuous recording of RyR2 activity in the presence of cytoplasmic 1 μmol/l Ca^{2+} and 2 mmol/l ATP obtained at +40 mV. At the beginning of the recording RyR2s were exposed to 50 μmol/l AMT which had been added to the cytoplasmic bath. Under these conditions AMT nearly fully activated the RyR2. Inter-burst periods are indicated by horizontal bars. The first arrow indicates when AMT was washed away by flowing AMT-free solution onto the bilayer. AMT-induced bursts continued to occur after perfusion albeit at a reduced frequency. The second arrow indicates when perfusion was turned off and AMT regained access to the RyR2. **(B)** Summary of burst frequency with respect to RyR2 opening, F_o, at different time points after perfusion was initiated. Data were obtained from a total of 9 perfusion cycles on 4 RyR2s. The solid curve shows an exponential fit with a decay constant of 17 ± 4 s and with $F_o = 11 \pm 4$ s^{-1} at time zero. **(C)** A control experiment

Molecular Pharmacology Fast Forward. Published on October 9, 2008 as DOI: 10.1124/mol.108.051490
This article has not been copyedited and formatted. The final version may differ from this version.

demonstrating that solution exchange occurs in ~ 1 s. Ten RyRs in the bilayer were initially exposed to 5 mmol/l Ca^{2+} in the cytoplasm (RyRs were partially inhibited by a low affinity Ca^{2+} inhibition). Perfusion was used to exchange the bath for one which contained < 1 nmol/l Ca^{2+} (5 mmol/l BAPTA, [Ca^{2+}] is too low to activate RyRs). On initiating solution exchange the RyR activity increased as the [Ca^{2+}] reduced to levels for maximal RyR activity (~ 100 μmol/l) and then RyRs deactivated once [Ca^{2+}] fell below 100 nmol/l.

Figure 6. Single channel recordings of RyR2s from sheep heart representative of 4 experiments obtained at -40 mV (A) and +40 mV (B). The dashes at the left of each record indicate the current baseline. The AMT concentrations in the *cis* bath are listed at the left of each trace and the open probability of the channels at the right. The *cis* bath also contained 2 mmol/l ATP and 1 μmol/l free Ca^{2+} (2 mmol/l BAPTA + 1 mmol/l $CaCl_2$).

Figure 7. AMT activates cardiac RyR2s isolated from *Casq2*$^{+/+}$ and *Casq2*$^{-/-}$ mice. The effects of AMT in the *cis* (cytoplasmic) bath were in the presence of 2 mmol/l ATP and 0.1 μmol/l free Ca^{2+} (4.5 mmol/l BAPTA + 1 mmol/l $CaCl_2$). The *trans* (luminal) bath contained 0.1 mM Ca^{2+} (**A, B**) Single channel recordings of RyR2s at +40 mV. The top traces show channel activity in the absence of AMT (control). The bottom three traces are continuous recordings obtained in the presence of 10 μmol/l AMT. The dashes at the left of each record indicate the current baseline and channel openings are upward transitions from the baseline. Amitriptyline induced long lasting openings of at least two conductance levels (**C**) Pooled results showing the relative effect (normalized to control levels) of 5-10 μmol/l of AMT on RyR2 open probability, P_o, mean open time, τ_o , and mean closed time, τ_c. The number of samples in the means is given in parentheses.

Molecular Pharmacology Fast Forward. Published on October 9, 2008 as DOI: 10.1124/mol.108.051490
This article has not been copyedited and formatted. The final version may differ from this version.

Figure 8. AMT exposure causes a concentration-dependent reduction in SR Ca^{2+} content in intact myocytes. (A) Representative examples of rapid caffeine application (10 mmol/l) to Fura-2 loaded myocytes exposed to increasing concentrations of AMT. Myocytes were incubated with respective concentration of AMT for at least 10 minutes before experiments. The height of the caffeine-induced Ca^{2+} transient was used as a measure of SR Ca^{2+} content. **(B)** Average values of SR Ca^{2+} content in myocytes exposed to increasing AMT concentrations (0, 0.5, 1, 3, 10, 30, 300 µmol/l). Note the concentration-dependent decrease in SR Ca^{2+} content in myocytes. Numbers indicate the number of myocytes examined for each drug concentration. *p<0.05 for comparison with 0 µmol/l AMT using *Student's t test*.

Figure 9. Spontaneous SR Ca^{2+}-release events (SCRs) in myocytes exposed to increasing AMT concentrations. (A) Representative examples of SCRs in a Fura-2 loaded myocytes exposed to 1 µmol/l AMT. Upon emptying the SR (rapid exposure to 10 mmol/l caffeine) the SCRs were abolished only to reappear once the SR refilled (*data not shown*). **(B)** Comparison of the incidence of SCRs in myocytes exposed to increasing AMT concentrations. Data represent the average number of SCRs/second during the recording period of 40 seconds. Note the significant increase in SCRs at 0.5 and 1 µmol/l AMT when compared to 0 µmol/l AMT. In contrast, at higher AMT concentrations (>3 µmol/l) there was a decrease in SCRs probably due to decrease in SR Ca^{2+} content (see Figure 8B). Numbers indicate the number of myocytes examined for each drug concentration. *p<0.05 for comparison with 0 µmol/l using *Student's t test*. **(C)** Dependence of SCR rates on SR Ca^{2+} content in myocytes exposed to 0 and 1 µmol/l AMT. SR Ca^{2+} content was altered by incubating myocytes in solutions with extracellular Ca^{2+}

Molecular Pharmacology Fast Forward. Published on October 9, 2008 as DOI: 10.1124/mol.108.051490
This article has not been copyedited and formatted. The final version may differ from this version.

concentrations ranging from 2 to 5 mmol/l. As expected, SCR rates increased with increased SR Ca^{2+} content. Note that 1 µmol/l AMT significantly increased rates of SCR across a wide range of SR Ca^{2+} loads. 0 µmol/l AMT, n=99; 1 µmol/l AMT, n=82; *p<0.05, **p<0.01, ***p<0.001 using *Student's t test*.

Figure 10. AMT induces SCRs in absence of trans-sarcolemmal Ca^{2+} fluxes by increasing SR Ca^{2+} leak. (A) Representative examples of fluorescence records obtained from quiescent Fura-2 loaded myocytes exposed to 0 and 1 µmol/l AMT (left panel and right panel, respectively) in Na^+ and Ca^{2+} free Tyrode's solution which abolishes trans-sarcolemmal Ca^{2+} flux. Note that SCRs were more frequent in the AMT-exposed myocyte. As indicated, external solution was then rapidly changed to Na^+ and Ca^{2+} free Tyrode's solution containing 1 mmol/l tetracaine, a blocker of RyR2 channels. The resulting drop in the fluorescence record (arrow) represents an estimate of diastolic SR Ca^{2+} leak (see methods for details). **(B and C)** Comparison of SCRs rates **(B)** and SR Ca^{2+} leak **(C)** in myocytes exposed to 0 and 1 µmol/l AMT. Data represent the average number of SCRs/second during a recording period of 30 seconds for each myocyte. Note that 1 µmol/l AMT significantly increased both the rate of SCRs and Ca^{2+} leak even when trans-sarcolemmal Ca^{2+} fluxes are eliminated. **p<0.01, ***p<0.001 using *Student's t test*.

Figure 11. AMT accumulates in myocytes leading to higher intracellular concentrations. Myocytes were incubated with AMT (0-300 µmol/l) for 1 hour, washed three times to remove extracellular AMT and the amount of AMT retained intracellularly determined by LC/MS/MS after liquid phase extraction using imipramine as an internal standard (see methods for details). Each point represents 3 separate experiments. Note that intracellular concentrations of AMT are

approximately 5 times greater than that of the extracellular AMT concentrations in the bath, suggesting accumulation of AMT inside the cell.

Figure 12. Mg^{2+} restores SR Ca^{2+} content and prevents SCRs in AMT-exposed myocytes. **(A)** Average values of SR Ca^{2+} content in presence of low (1 mmol/l) and high (5 mmol/l) Mg^{2+} in myocytes exposed to 0, 1 and 10 µmol/l AMT. **(B)** Incidence of SCRs in myocytes exposed to 0, 1 and 10 µmol/l AMT in presence of low (1 mmol/l) and high (5 mmol/l) Mg^{2+}. Note that high Mg^{2+} (5 mmol/l) completely abolished the AMT-induced increase in SCRs. This suggests that the stabilizing effect of Mg^{2+} on RyR2 channels preferentially antagonizes the action of AMT. **p<0.01, ***p<0.001 using *Student's t test*.

Molecular Pharmacology Fast Forward. Published on October 9, 2008 as DOI: 10.1124/mol.108.051490
This article has not been copyedited and formatted. The final version may differ from this version.

TABLE 1. The effects of cytoplasmic [Ca^{2+}] and [Mg^{2+}] on the properties of AMT induced bursts in RyR2s from sheep heart. The cytoplasmic bath contained 2 mmol/l ATP plus the indicated free concentrations of Ca^{2+} and Mg^{2+}. Frequency of bursts was derived from either the total time between bursts (F) or the total open time between bursts (F_o).). n refers to the number of separate recordings from which the data was obtained.

Cytoplasmic conditions	F/(μmol/l), (μmol/l)s^{-1}	F_o/(μmol/l) (μmol/l)s^{-1}	P_o	Duration s	τ_o ms	n
1 μmol/l Ca^{2+}	$(1.2 \pm 0.3).10^{-2}$	0.27 ± 0.03	0.044	4.2 ± 1.4	3.7± 1.4	6
0.1 μmol/l Ca^{2+}	$(16 \pm 2).10^{-4}$	0.18 ± 0.06	0.008	7.8 ± 1.7	3.9± 1.2	3
0.1 μmol/l Ca^{2+}, 220 μmol/l Mg^{2+}	$(4 \pm 2).10^{-4}$	0.32 ± 0.15	0.0013	2.2 ± 1.4	2.1± 0.7	3

Molecular Pharmacology Fast Forward. Published on October 9, 2008 as DOI: 10.1124/mol.108.051490
This article has not been copyedited and formatted. The final version may differ from this version.

Figure 1

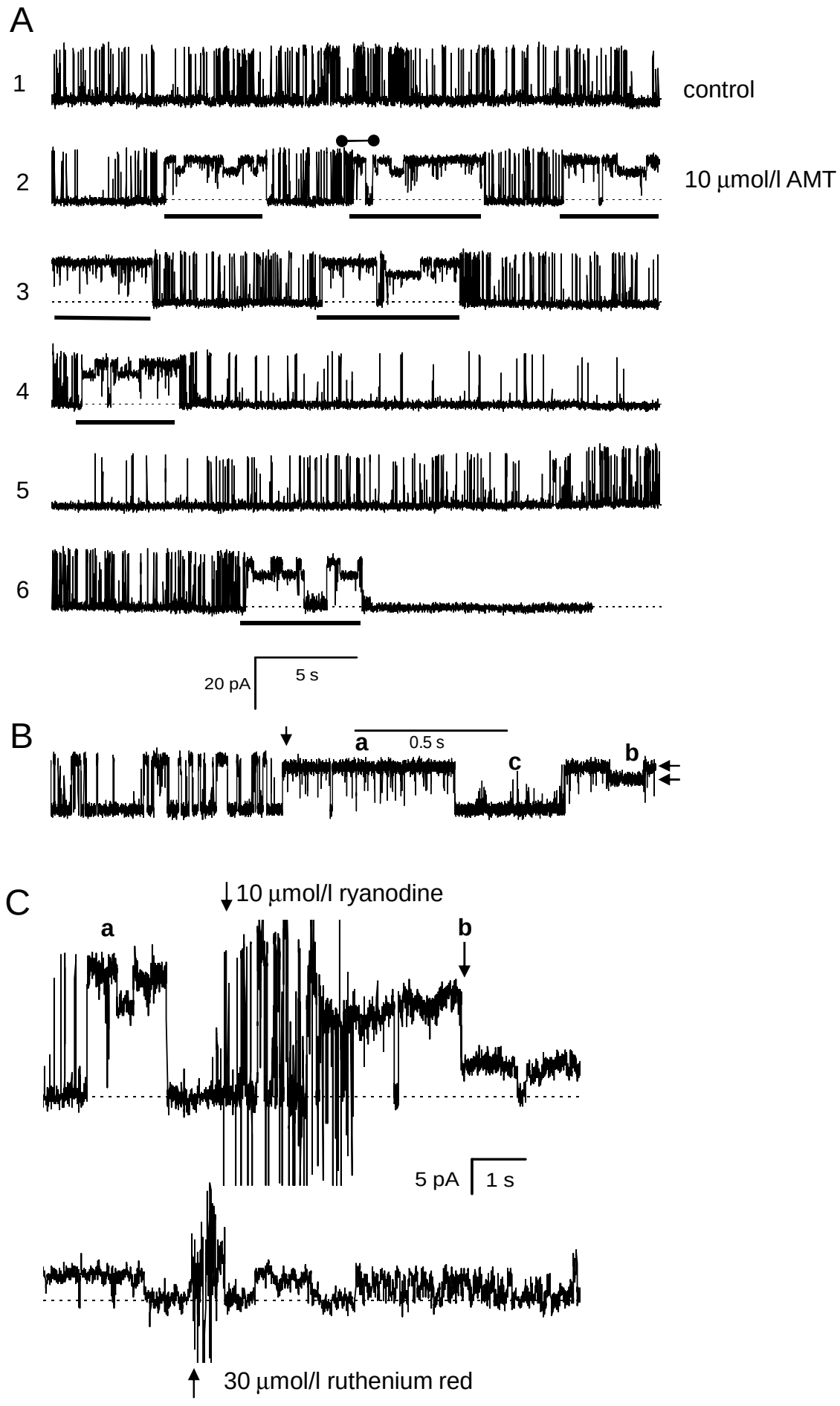

Molecular Pharmacology Fast Forward. Published on October 9, 2008 as DOI: 10.1124/mol.108.051490
This article has not been copyedited and formatted. The final version may differ from this version.

Figure 2

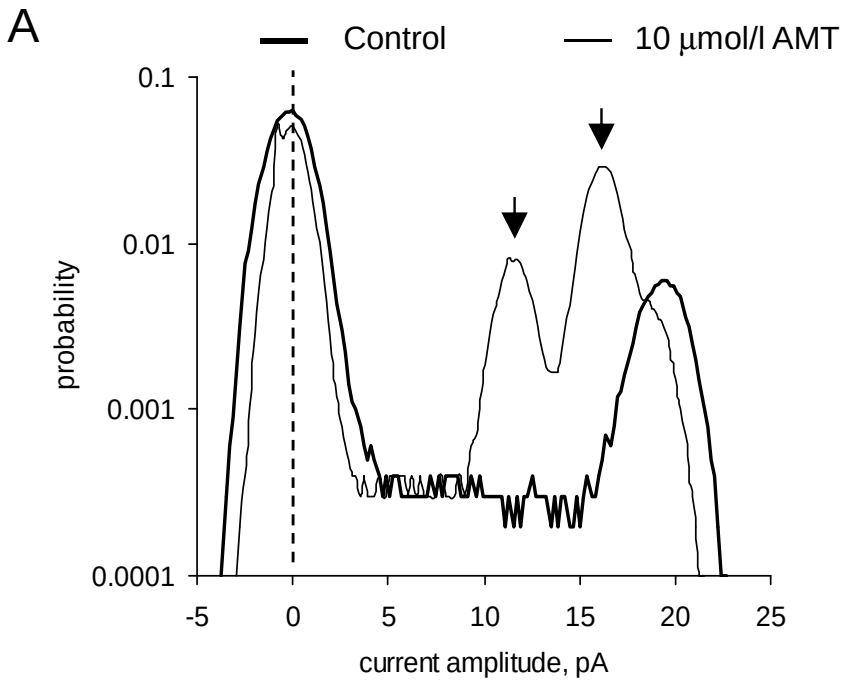

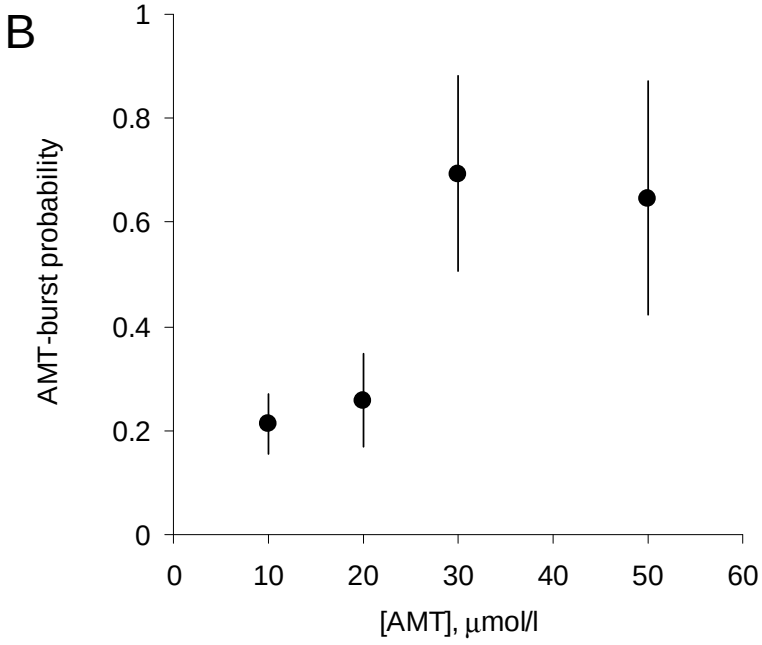

Molecular Pharmacology Fast Forward. Published on October 9, 2008 as DOI: 10.1124/mol.108.051490
This article has not been copyedited and formatted. The final version may differ from this version.

Figure 3

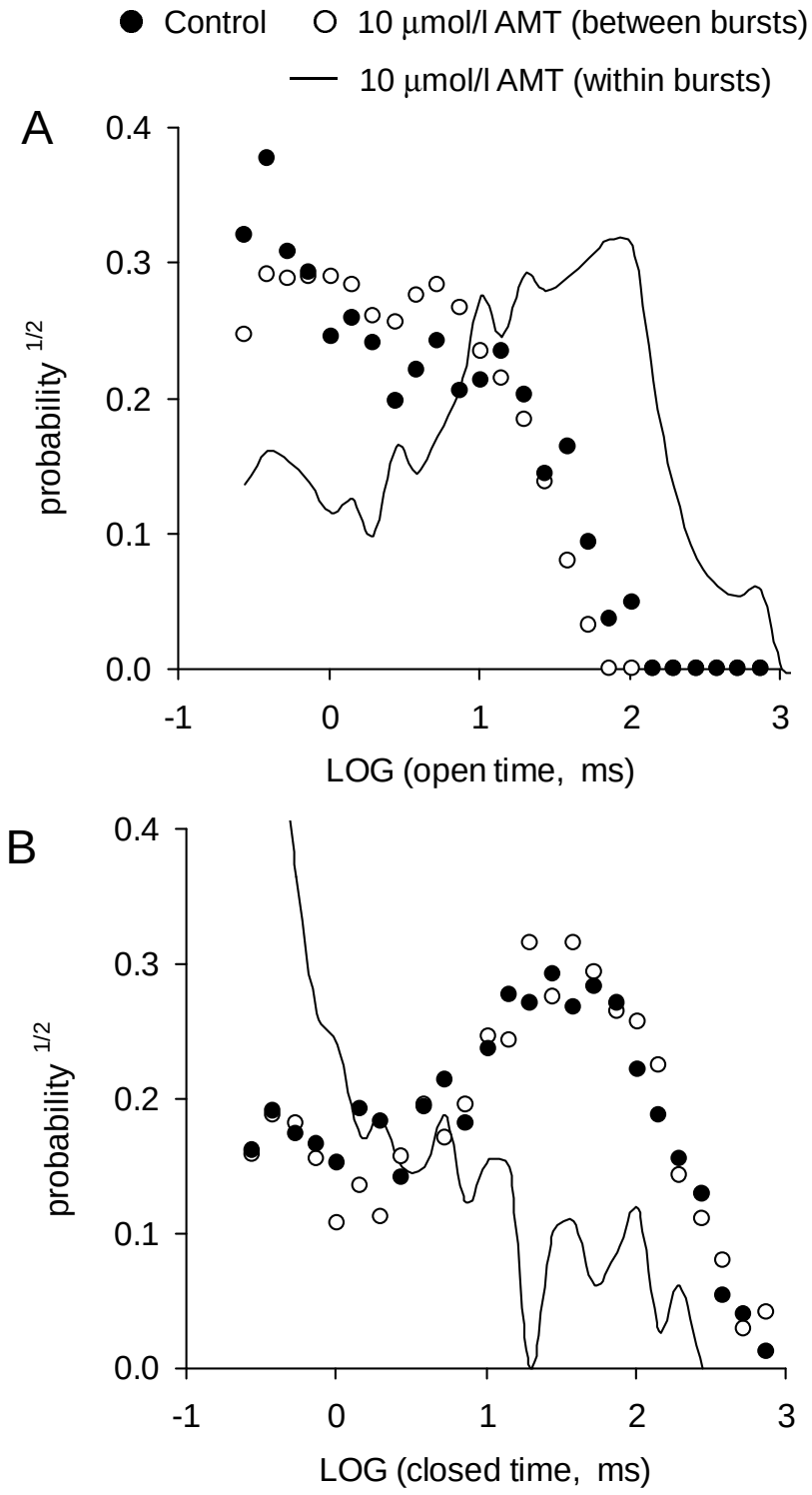

Molecular Pharmacology Fast Forward. Published on October 9, 2008 as DOI: 10.1124/mol.108.051490
This article has not been copyedited and formatted. The final version may differ from this version.

Figure 4

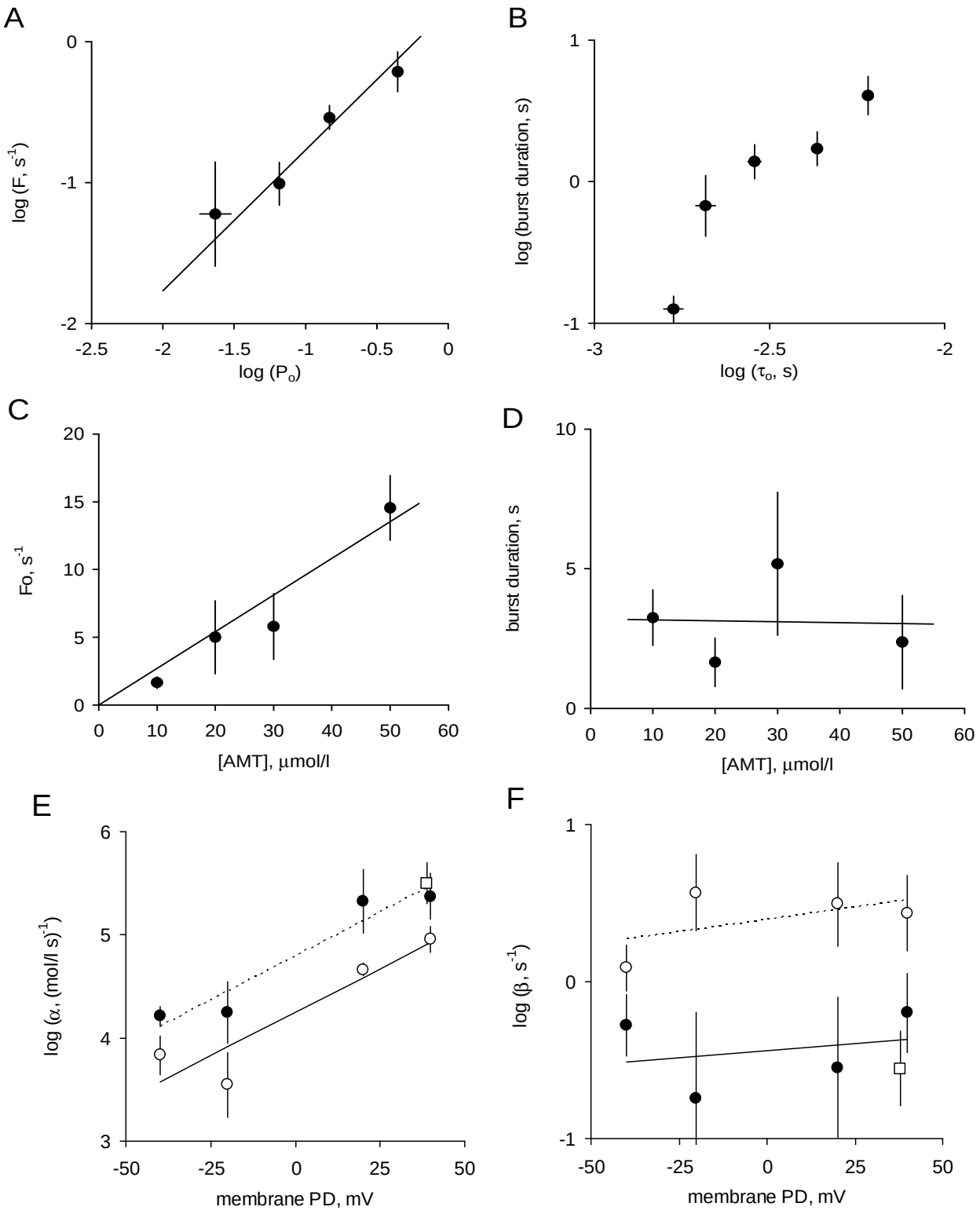

Molecular Pharmacology Fast Forward. Published on October 9, 2008 as DOI: 10.1124/mol.108.051490
This article has not been copyedited and formatted. The final version may differ from this version.

Figure 5

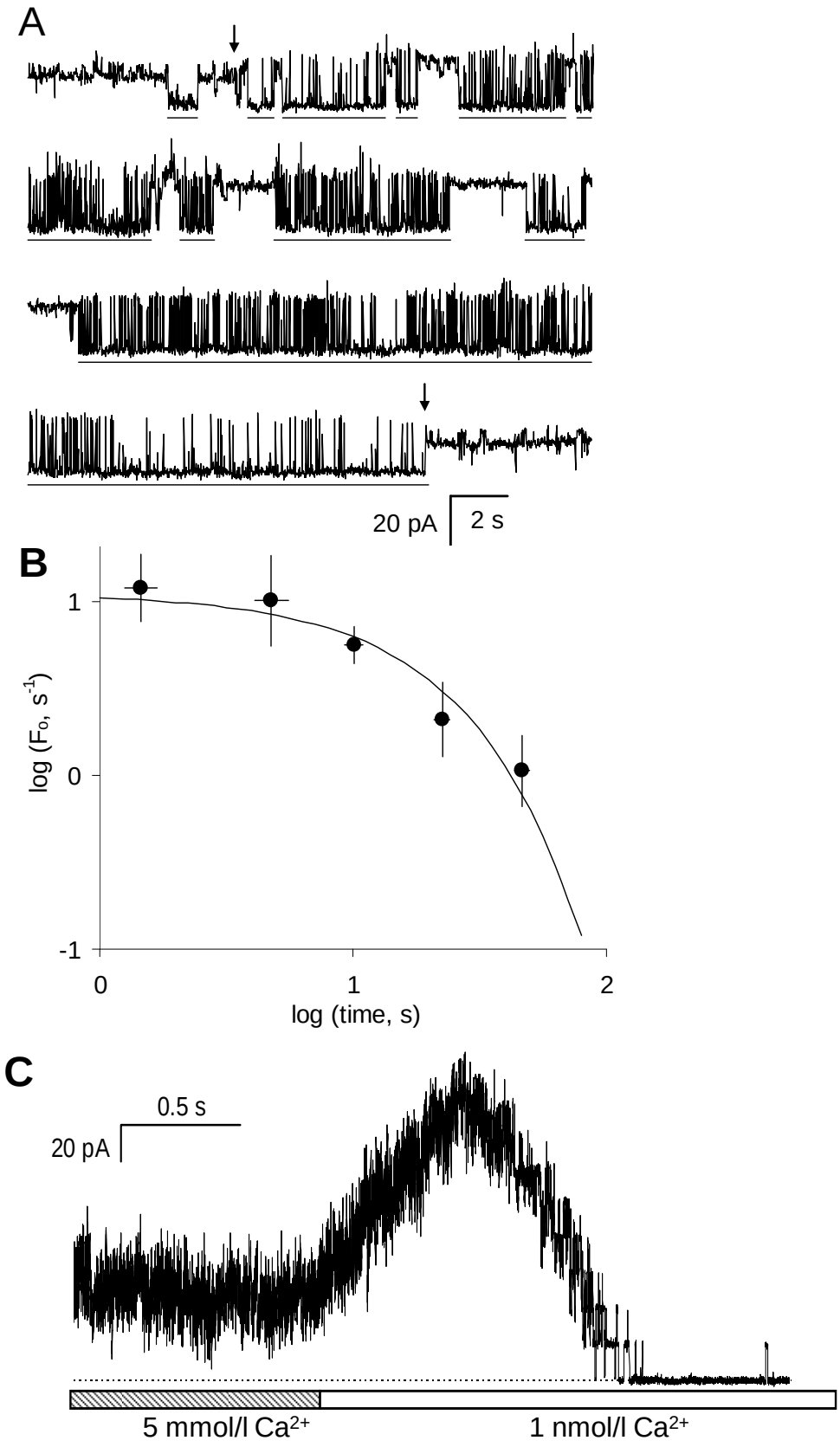

Molecular Pharmacology Fast Forward. Published on October 9, 2008 as DOI: 10.1124/mol.108.051490
This article has not been copyedited and formatted. The final version may differ from this version.

Figure 6

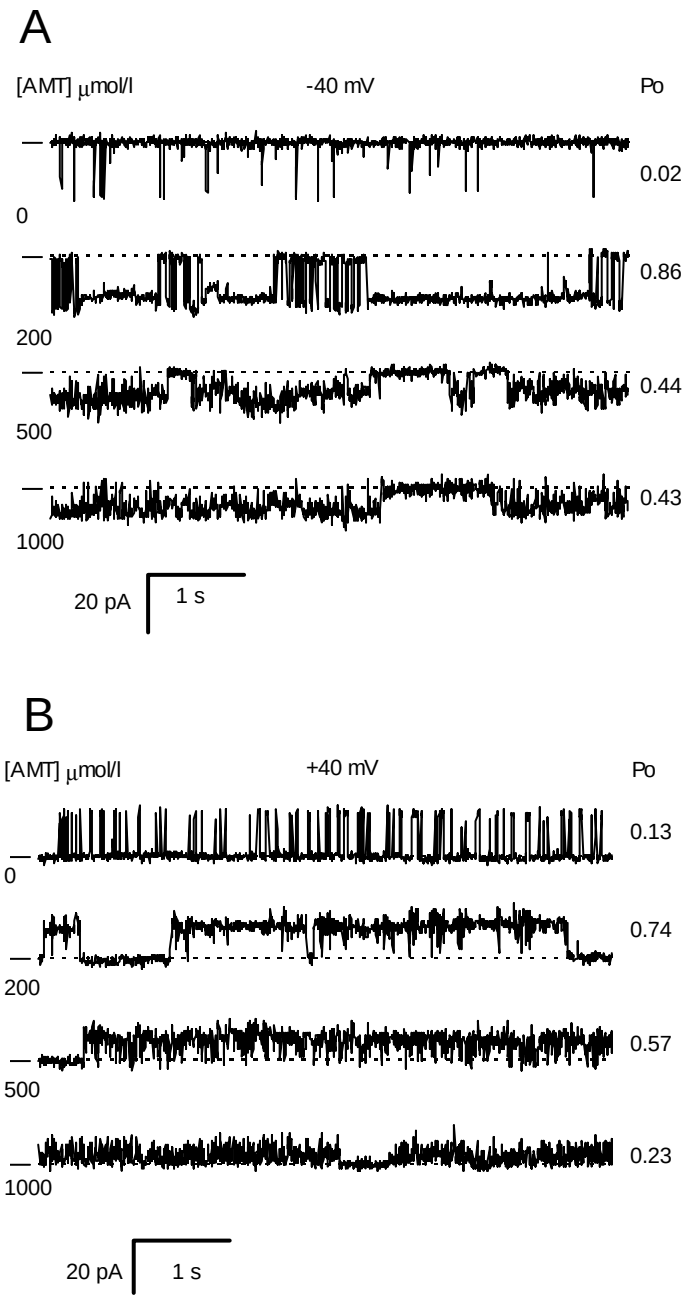

Molecular Pharmacology Fast Forward. Published on October 9, 2008 as DOI: 10.1124/mol.108.051490
This article has not been copyedited and formatted. The final version may differ from this version.

Figure 7

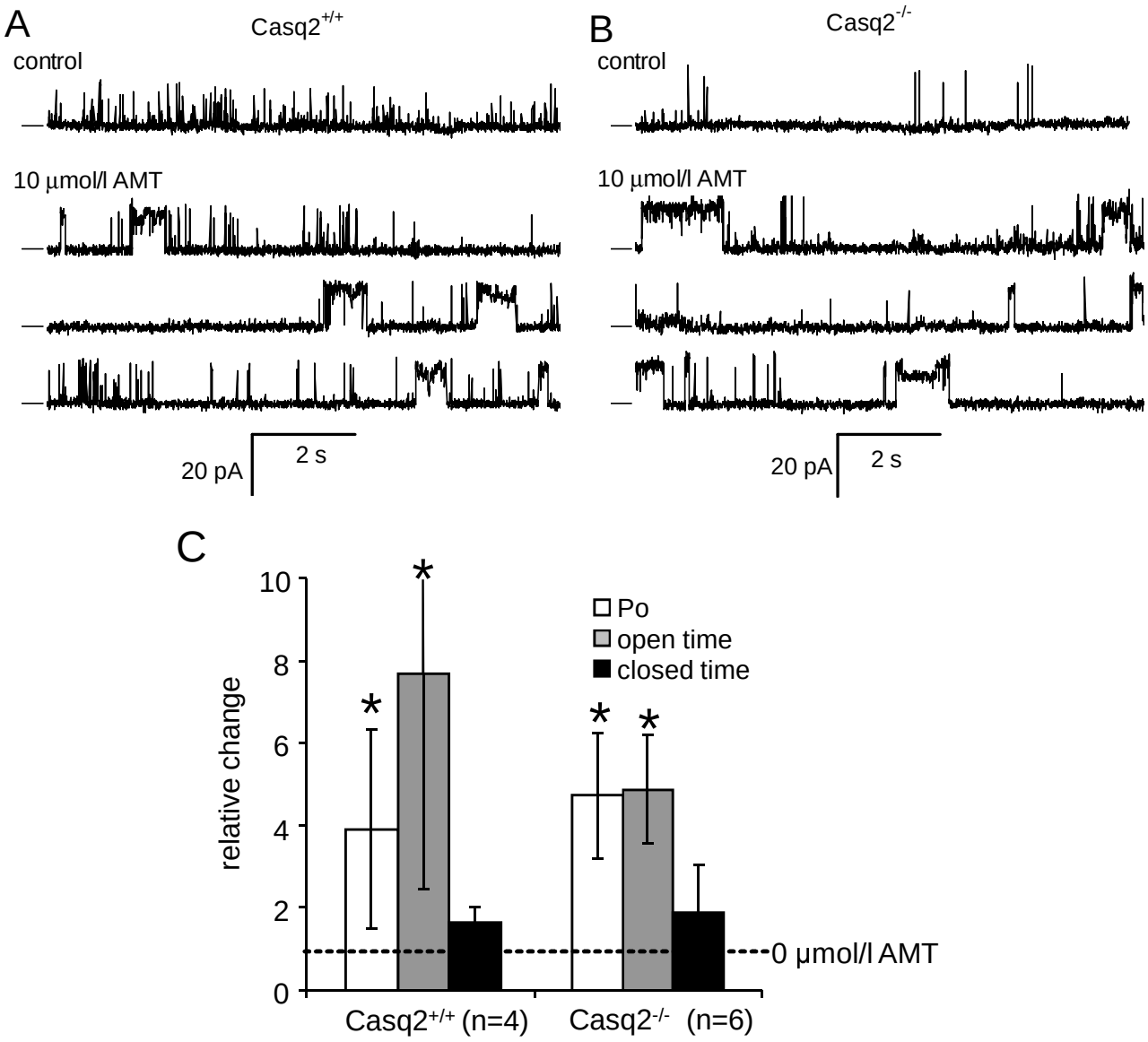

Molecular Pharmacology Fast Forward. Published on October 9, 2008 as DOI: 10.1124/mol.108.051490
This article has not been copyedited and formatted. The final version may differ from this version.

Figure 8

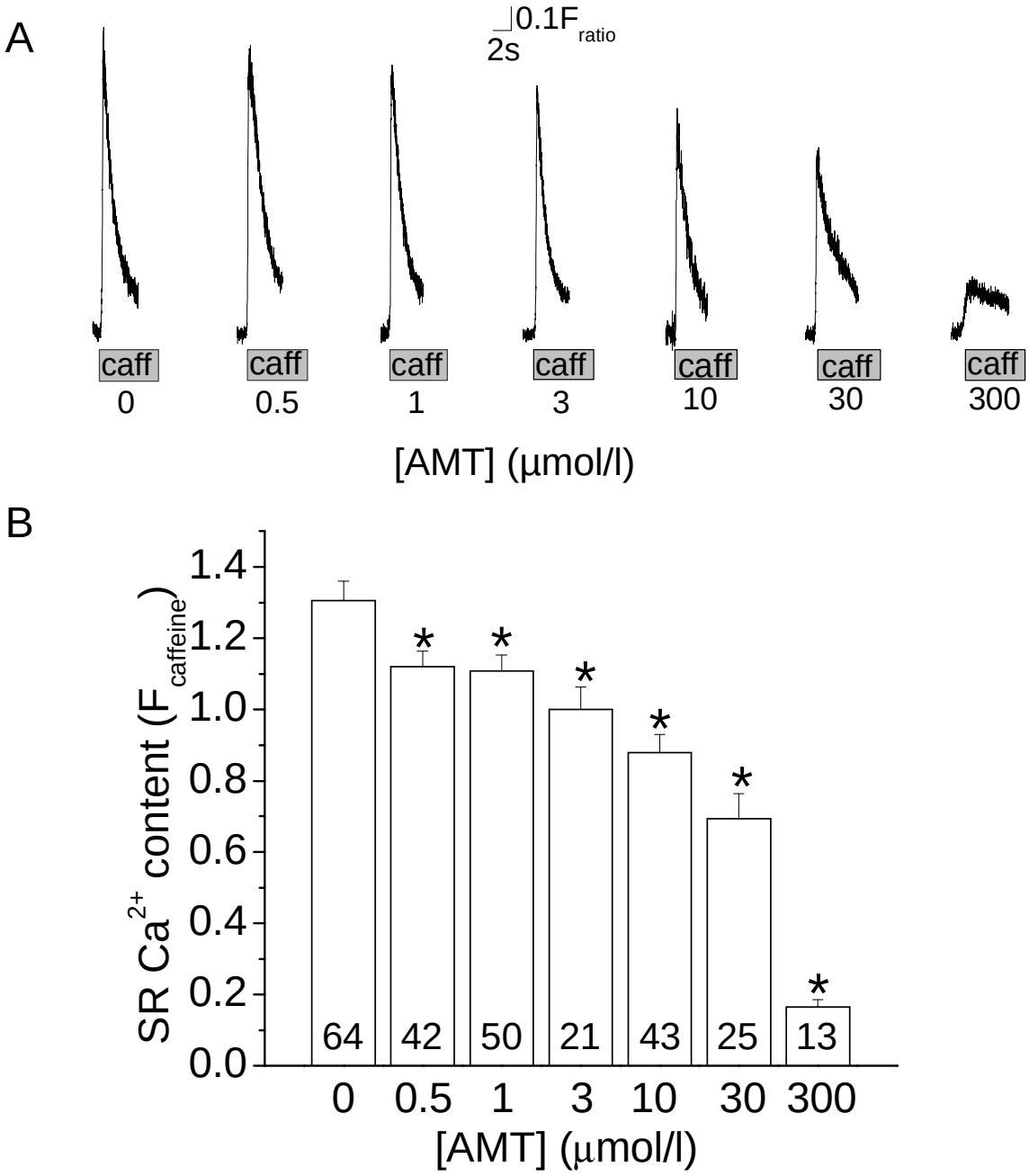

Molecular Pharmacology Fast Forward. Published on October 9, 2008 as DOI: 10.1124/mol.108.051490
This article has not been copyedited and formatted. The final version may differ from this version.

Figure 9

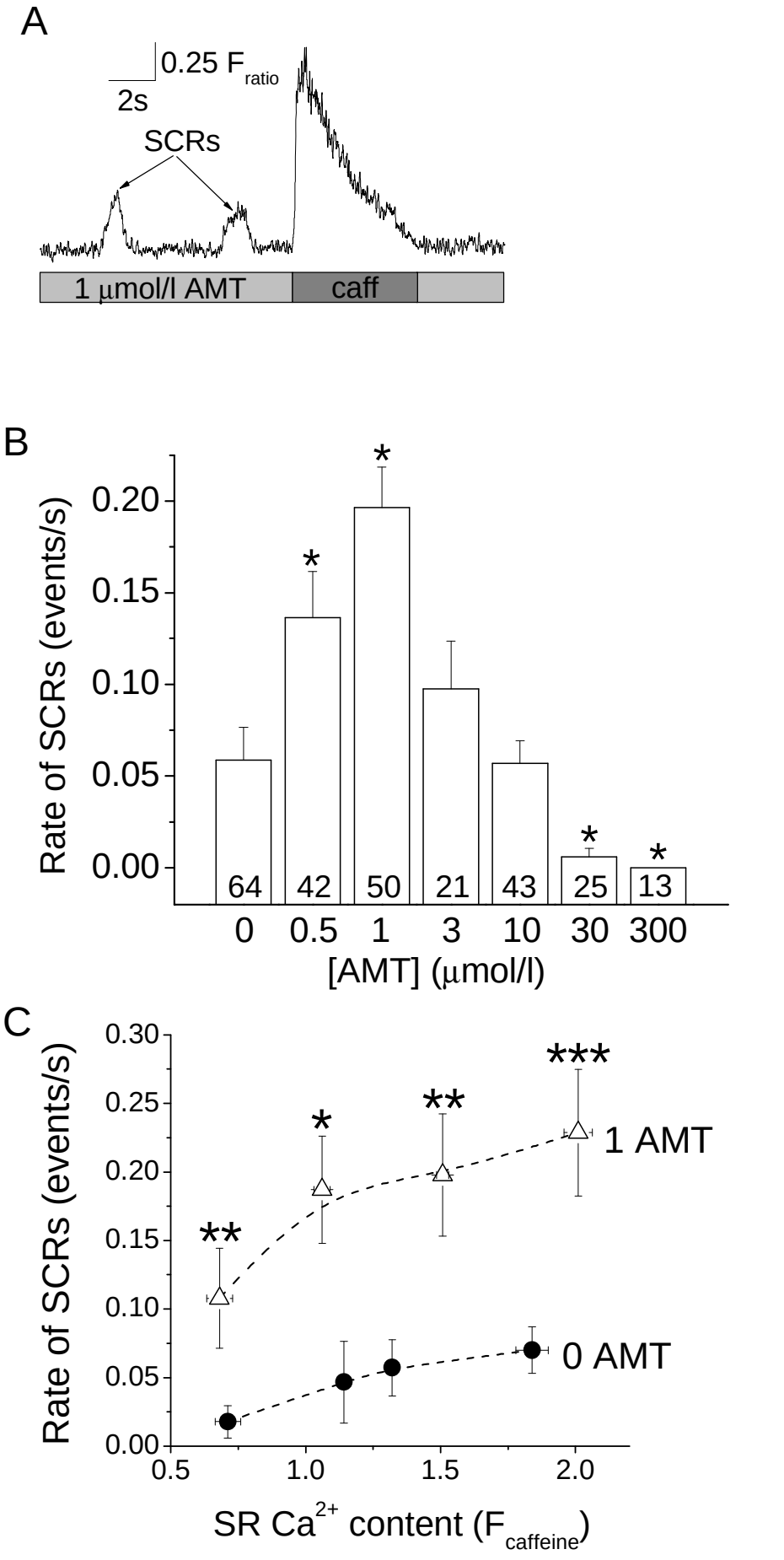

Molecular Pharmacology Fast Forward. Published on October 9, 2008 as DOI: 10.1124/mol.108.051490
This article has not been copyedited and formatted. The final version may differ from this version.

Figure 10

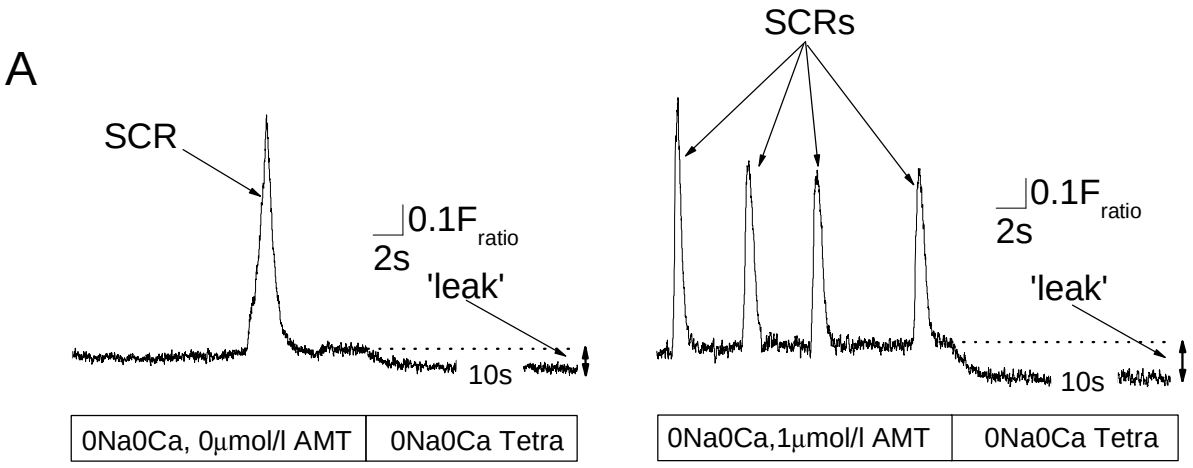

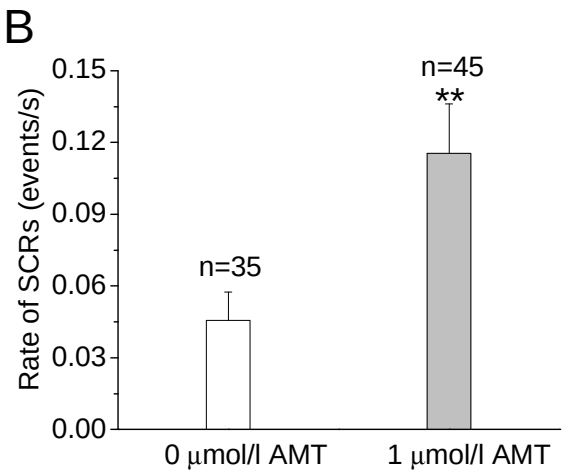

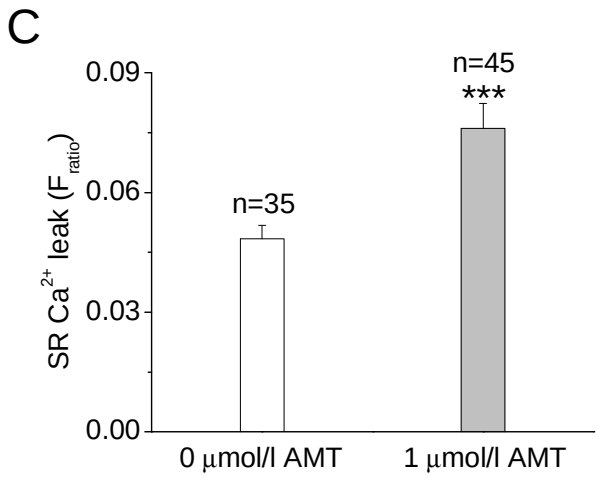

Molecular Pharmacology Fast Forward. Published on October 9, 2008 as DOI: 10.1124/mol.108.051490
This article has not been copyedited and formatted. The final version may differ from this version.

Figure 11

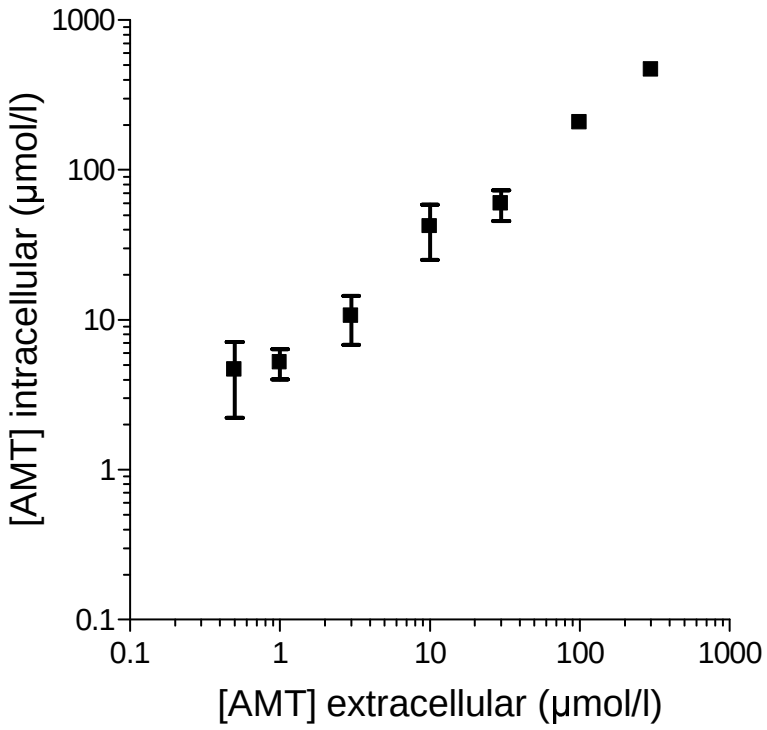

Molecular Pharmacology Fast Forward. Published on October 9, 2008 as DOI: 10.1124/mol.108.051490
This article has not been copyedited and formatted. The final version may differ from this version.

Figure 12